

**Editorial Summary:** This Perspective analyzes the most common maturation and assessment techniques for *in vitro* hiPSC-derived cardiomyocyte models and makes recommendations for standardizations in this field.

## Induced pluripotent stem cell-derived cardiomyocyte *in vitro* models: benchmarking progress and ongoing challenges

### Authors

Jourdan K. Ewoldt<sup>1†</sup>, Samuel J. DePalma<sup>2†</sup>, Maggie E. Jewett<sup>2</sup>, M. Çağatay Karakan<sup>1,3,4</sup>, Yih-Mei Lin<sup>5</sup>, Paria Mir Hashemian<sup>3,4</sup>, Xining Gao<sup>1,6,7</sup>, Lihua Lou<sup>8</sup>, Micheal McLellan<sup>1,7</sup>, Jonathan Tabares<sup>9</sup>, Marshall Ma<sup>3,4</sup>, Adriana C. Salazar Coariti<sup>10</sup>, Jin He<sup>9</sup>, Kimani C. Toussaint, Jr.<sup>10,11</sup>, Thomas G. Bifano<sup>3,4</sup>, Sharan Ramaswamy<sup>5</sup>, Alice E. White<sup>1,3,4,12,13</sup>, Arvind Agarwal<sup>8</sup>, Emma Lejeune<sup>3</sup>, Brendon M. Baker<sup>2\*</sup>, Christopher S. Chen<sup>1,7\*</sup>

† Authors contributed to this work equally.

\*Corresponding author. Email: chencs@bu.edu (C.S.C), bambren@umich.edu (B.M.B)

### Affiliations

1. Department of Biomedical Engineering, Boston University, Boston, MA 02215, USA
2. Department of Biomedical Engineering, University of Michigan, Ann Arbor, MI 48109, USA
3. Department of Mechanical Engineering, Boston University, Boston, MA 02215, USA
4. Photonics Center, Boston University, Boston, MA 02215, USA
5. Department of Biomedical Engineering, Florida International University, Miami, FL 33174, USA
6. Harvard-MIT Program in Health Sciences and Technology, Institute for Medical Engineering and Science, Massachusetts Institute of Technology, Cambridge, MA 02139, USA
7. Wyss Institute for Biologically Inspired Engineering, Harvard University, Boston, MA 02115, USA
8. Department of Mechanical and Material Engineering, Florida International University, Miami, FL 33174, USA
9. Department of Physics, Florida International University, Miami, FL 33199, USA
10. School of Engineering, Brown University, Providence, RI 02912, USA
11. Brown-Lifespan Center for Digital Health, Providence, Rhode Island 02912, USA.
12. Division of Materials Science and Engineering, Boston University, Boston, MA 02215, USA
13. Department of Physics, Boston University, Boston, MA 02215, USA

### Abstract

Recent innovations in differentiating cardiomyocytes from human induced pluripotent stem cells (hiPSCs) have unlocked a viable path to creating *in vitro* cardiac models. Currently, hiPSC-derived cardiomyocytes (hiPSC-CMs) remain immature, leading many in the field to explore approaches to enhance cell and tissue maturation. Here, we systematically analyzed 300 studies using hiPSC-CM models to determine common fabrication, maturation, and assessment techniques used to evaluate cardiomyocyte functionality and maturity and compiled the data into an open access database. Based on this analysis, we present the diversity of, and current trends in, *in vitro* models and highlight the most common and promising practices for functional assessments. We further analyzed outputs spanning structural maturity, contractile function, electrophysiology, and gene expression and note field-wide improvements over time. Finally, we discuss opportunities to collectively pursue the shared goal of hiPSC-CM model development, maturation, and assessment that we believe are critical to engineering mature cardiac tissue.

### Main Text

#### I. Introduction

##### A. Utility of hiPSC-cardiomyocyte models

The average cost to bring a new pharmaceutical to the market in the United States is estimated at more than one billion dollars<sup>1</sup>, and approximately 10% of pharmaceuticals worldwide have been withdrawn due to adverse cardiovascular side effects<sup>2</sup>. This high failure rate is in part due to the relative difficulty in predicting which drugs will have adverse cardiac effects: primary human cardiomyocytes (CMs) are difficult to obtain and rapidly dedifferentiate *in vitro*, rendering them incapable of faithfully detecting anything but acute effects of pharmaceuticals on the heart<sup>3</sup>. On the other hand, while animal models can reveal cardiotoxic and arrhythmogenic activity of pharmaceuticals, there are key differences in cardiac biology between species that limit their ability to fully predict the potential for adverse cardiovascular effects in humans<sup>4</sup>.

The advent of the first differentiation protocol of human embryonic stem cells (hESCs) into CMs in 1993 enabled researchers to study human cardiomyocytes *in vitro* in ways not possible with primary CMs<sup>5</sup>. In 2007, the first human induced pluripotent stem cells (hiPSCs) were generated. Derived from skin or blood cells and reprogrammed into a pluripotent state, these cells can be patient-derived and can be differentiated into CMs without the ethical challenges associated with sourcing hESCs<sup>6</sup>. Thus, this approach allows for the testing of pharmaceutical cardiovascular effects of in a more physiologically relevant model<sup>7</sup>.

The use of hiPSC technology to generate human CMs has also enabled the study of myocardial physiology and pathobiology. Inherited cardiomyopathies, such as hypertrophic, dilated, and arrhythmogenic cardiomyopathies (HCM, DCM, ACM), affect 1/500, 1/250, and 1/2,000-5,000 of the population, respectively<sup>8</sup>, and are caused by over 100 genes and over 1,000 possible genetic mutations<sup>9-11</sup>. Patient-derived hiPSC-CM models of genetic cardiomyopathies and CRISPR/Cas9 edited hiPSC-CMs have thus been used to recapitulate disease *in vitro*, to shed light on new disease mechanisms, and to establish the promise for gene-editing strategies to correct these diseases<sup>12-21</sup>. Additionally, hiPSC-CMs have shown promise as regenerative therapies for patients with heart failure<sup>22,23</sup>.

However, despite all the promise associated with hiPSC-CMs, the overall immaturity of hiPSC-CMs limits their utility. Fetal-like gene expression patterns, immature structure and function, and non- or sub-physiologic electromechanical activity are all significant caveats to the conclusions drawn from studies using these cells to test pharmaceuticals or model disease states and are major hurdles for using these cells in regenerative or reparative therapies.

## B. Immaturity of hiPSC-cardiomyocyte models

hiPSC-CMs typically exhibit immature structural phenotypes, including disorganized myofibrils, fewer mitochondria, and poor co-localization of calcium channels and ryanodine receptors that ultimately impair the functionality of hiPSC-CMs as compared to adult cardiomyocytes (Table 1)<sup>24</sup>. Additionally, engineered cardiomyocytes mainly rely on glycolysis for energy, rather than more efficient energy production from oxidative phosphorylation utilized by adult cardiomyocytes. Functionally, human adult cardiomyocytes exhibit a resting membrane potential and conduction velocity of approximately -90 mV and 30-100 cm/s<sup>25</sup>, respectively, while very few hiPSC-CM models have shown a resting membrane potential below -80 mV<sup>22,26-30</sup> or a conduction velocity above 40 cm/s<sup>22,28,31</sup>. Additionally, the twitch force of adult human cardiomyocytes is 25-44 mN/mm<sup>2</sup><sup>32</sup>, and only a few hiPSC-CM engineered constructs have achieved this level of contractility<sup>21,33</sup>.

In the past decade, there have been great strides made toward understanding how to further mature hiPSC-CMs by combining knowledge from diverse fields. In achieving these advances, researchers have used many different cell lines, differentiation protocols, maturation techniques, and functional assessments, making it challenging for the field to make head-to-head comparisons between studies. As the field of cardiac tissue engineering itself matures, standardized benchmarking across the field will be essential to extracting key findings and applying them toward future advances.

To assess the current state of the art, we sought to systematically analyze a breadth of studies utilizing hiPSC-CMs by extracting protocols and functional assessment metrics. In synthesizing the key findings from these analyses, here we provide guidance on best practices for generating and assessing the maturity

of hiPSC-CMs with the goal of fostering a transparent discussion toward convergence amongst the community to progress toward engineering adult-like hiPSC-CMs.

## II. Methodology

Across over 2,000 studies utilizing hiPSC-CMs from 2016-2022, there exists high variability in differentiation protocols, maturation strategies, and assessment of cell or tissue functionality. To understand the nature of this variability, we systematically analyzed 300 studies using hiPSC-CM models and compiled data on these components. Using a PubMed search for “(((induced pluripotent stem cells) OR (iPSC)) AND ((cardiomyocyte) OR (cardiomyocytes) OR (iPSC-CM) OR (iPSC-CMs) OR (induced pluripotent stem cell-cardiomyocytes) OR (induced pluripotent stem cell-CMs))) AND ((engineered heart tissue) OR (cardiac microtissue) OR (maturation) OR (mature))” we identified 846 potential publications for analysis. We eliminated publications focusing on atrial differentiation due to relatively limited work in this space and focused our benchmarking on ventricular cardiomyocytes. We also eliminated publications that were solely focused on disease modeling but included disease modeling publications in which maturation techniques (the primary focus of our analysis) were utilized in model development. To capture overall trends in the field, we focused on 300 publications. This included the top 100 cited publications from the 846 potential publications based on citation numbers reported by the Web of Science database as of 2022, 100 randomly selected publications from the potential publications, and 100 additional hiPSC-CM publications that were manually selected from references in recent high impact reviews on cardiac tissue engineering or top search results for “iPSC-cardiomyocytes” on Google Scholar.

After accumulating and analyzing data reported from these publications, we analyzed functional outputs in structural, contractile, calcium handling, electrophysiology, gene expression, and metabolic assessments to identify patterns in the effects of model parameters on cardiac maturation. Graphs depicting functional outputs show mean  $\pm$  standard error of the mean (SEM) unless otherwise noted. Data were assessed with a one-way ANOVA that was corrected for multiple comparisons using a Tukey test with a 95% confidence level. All data used for these analyses can be found in Supplementary Data Set 1<sup>34</sup>.

## III. Current approaches to engineer hiPSC-CM *in vitro* models

### A. hiPSC culture and differentiation

With the widespread adoption of hiPSC-CMs in the field of cardiac tissue engineering, more hiPSC lines are being generated and used in studies to capture global diversity and generate patient-specific models. Here, we compiled information on the most commonly used hiPSC lines and hiPSC-CM differentiation protocols within the field.

#### *hiPSC lines*

A major source of variability across studies is the choice of hiPSC lines. Over 200 different hiPSC-lines were used across the analyzed studies. Over two-thirds of these studies used only one healthy control hiPSC line and thus failed to assess how different hiPSC lines may influence study findings (Fig. 1a). Of the 15 most used hiPSC lines across the papers analyzed (Fig. 1b), two-thirds have a female genetic background and only six have ancestral information available (Supplementary Table 1). Four of these 15 lines are hiPSC lines that are commercially differentiated into cardiomyocytes (Fig. 1b). Of note, Cor.4U cardiomyocytes that were used in 5% of studies we analyzed were found to be derived from hESCs, rather than hiPSCs, which are the focus of this review<sup>35</sup>. The most frequently reported lines that are not commercially differentiated include WTC11, IMR-90, DF19-9-11T.H, PGP1, 253G1, Gibco episomal line, 201B7, BJ1, SCVI-273, C25, and ATCC, (Fig. 1b). It has been shown that the genetic background of hiPSC lines impacts the maintenance of hiPSC pluripotency<sup>36</sup> and influences transcriptional variation<sup>37</sup> that could ultimately impact the differentiation and function of derived hiPSC-CMs<sup>38</sup>, highlighting the importance of including hiPSCs from diverse genetic backgrounds.

### *hiPSC differentiation to cardiomyocytes*

hiPSC culture medium can also influence the maintenance of hiPSC pluripotency and self-renewal<sup>39</sup>. Over 55% of publications utilized one of two commercially available hiPSC culture media as backbone medium: mTeSR-1 (STEMCELL Technologies) or Essential 8 Medium (E8) (Gibco) (Supplementary Data Set 1). During and after differentiation, the backbone culture medium was typically changed to RPMI-1640 (>50%), StemPro-34 (~5%), or commercially available kits. Supplements and additives such as B-27 (>50% of publications), L-ascorbic acid, albumin, L-glutamine, HEPES, and more were added to some cultures (Supplementary Data Set 1). Additionally, the matrix (if any) that hiPSCs are seeded on during and after differentiation has been found to impact hiPSC-CM purity and maturation<sup>40,41</sup>. Matrigel (~30%), gelatin (~20%), and fibronectin (~15%) were the most commonly reported matrices used for hiPSC culture (Supplementary Data Set 1).

While most protocols used to generate cardiomyocytes are based on temporal modulation of the Wnt signaling pathway<sup>42</sup>, adjustments to differentiation parameters are often required for successful CM differentiation across hiPSC lines<sup>43</sup> (Fig. 1d). Of the analyzed studies, CHIR9901 was the most commonly employed Wnt agonist used to initiate the differentiation process (used in >60% of studies analyzed). CHIR9901 was typically added to hiPSCs at ~80-90% confluence for 24 hours from Day 0 to about Day 1. Subsequent Wnt pathway inhibition via IWR-1, IWP-2, or IWP-4 was conducted from approximately Day 3 to Day 4 of differentiation. Insulin was typically added on Day 7 of differentiation. The use of metabolic selection to improve the purity of hiPSC-CMs<sup>44</sup> was only reported in one-third of the publications. Of these publications, about 70% removed glucose from the media and supplemented the media with lactate in order to starve non-myocytes.

While many studies failed to quantify hiPSC-CM purity following differentiation, over half of the studies reported using either flow cytometry or immunohistochemistry for cardiac-specific markers, such as cardiac troponin T (cTnT) or  $\alpha$ -actinin, to quantify the percentage of successfully differentiated hiPSCs (Fig. 1c). The average reported purity of cardiomyocytes was 84%.

Overall, similar differentiation protocols are used across the field; however, variations in timing and concentration of Wnt agonists/antagonists appear to be necessary for successful CM differentiation of different lines<sup>43</sup>. Additional variability arises from differences in culture techniques across groups. While we acknowledge the challenges associated with controlling for these variables, it would be advantageous for the field to reduce variability in differentiation protocols where possible. As a start, more studies should adopt a common differentiation protocol as a comparator to their group's traditional protocol and report the purity of their hiPSC-CMs. Purity is important not only when interpreting studies but also to provide additional assurances that non-CMs are not unknowingly impacting downstream functional outputs. Identifying and reporting the common non-CM cell populations that arise during differentiation could also aid in optimizing differentiation protocols to improve differentiation efficiency.

## **B. Platforms used to study hiPSC-CMs**

Following the differentiation of hiPSCs into CMs, these cells are typically incorporated into a variety of culture platforms to study their function, ranging from simple, high-throughput platforms to more complex bioreactor-like systems, many of which require engineering expertise and/or the inclusion of other cell types.

### *2D platforms*

A variety of platforms have been used to generate hiPSC-CM models for studying hiPSC-CM maturation, disease progression, and drug toxicity. These models can broadly be divided into 2D vs. 3D tissue platforms. 2D platforms are more commonly used than 3D tissue platforms due to their accessibility and higher throughput readouts. Additionally, 2D platforms facilitate the use of imaging and higher resolution analysis techniques to study cardiomyocyte structure and function. Across both 2D and 3D tissues, the most used culture platform for hiPSC-CMs was extracellular matrix (ECM)-coated glass or plastic substrates (60%) (Fig. 2a). While fibronectin or Matrigel are typically coated onto culture surfaces

to facilitate cell adhesion, stromal cell-derived ECM has recently been reported to improve the maturation of hiPSC-CMs<sup>40</sup>.

Recent improvements to 2D platforms have focused on providing topographical cues to hiPSC-CMs to drive CM alignment, mimicking the organization of the native myocardium. This alignment has been achieved by culturing CMs on micropatterned rectangles or lines<sup>21,27,45-55</sup>, electrospun scaffolds composed of aligned polymeric fibers<sup>56-64</sup>, grooved substrates<sup>65-70</sup>, and 3D-printed anisotropic scaffolds<sup>71-73</sup>. Additionally, several studies have cultured hiPSC-CMs on elastomeric surfaces that better recapitulate the mechanics of the native myocardium<sup>74-79</sup>. These substrates are typically made from hydrogels or elastomers, including polyacrylamide<sup>53-55,80,81</sup> or polydimethylsiloxane (PDMS)<sup>28,82-84</sup>, respectively. While 2D platforms can provide insights into the effect of specific parameters (i.e. substrate stiffness and ligand type/density) on cardiomyocytes, they are difficult to maintain in long-term culture and do not accurately recapitulate the complex structure and dimensionality of native tissue. Thus, they are limited in their ability to mimic specific aspects of development, physiology, and disease.

### *3D platforms*

3D hiPSC-CM tissues have become more widespread as they more accurately recapitulate the 3D architecture of the cardiac microenvironment in which CMs normally function. The majority of 3D-cardiac microtissues studied are considered scaffold-free (Fig. 2b). An example of scaffold-free microtissues include spheroid cultures, which have been used as a high-throughput assay to test the effects of non-cardiomyocytes on tissue stability and maturation. Other 3D hiPSC-CM tissues require the addition of ECM proteins to facilitate tissue assembly. The most common ECM proteins used include fibrin, collagen, Matrigel, or some combination of these materials. Additionally, a handful of groups have explored the use of decellularized ECM<sup>85-88</sup> and synthetic hydrogels made of materials such as polyethylene glycol<sup>71,89</sup> to generate cardiac microtissues. Further, the culture media used to maintain these tissues has a significant impact on the system, with over 80 combinations of media components utilized. More than one-third of the 3D hiPSC-CM models were cultured in media containing serum, despite its limited translational potential. 3D hiPSC-CMs are more physiologically relevant overall, but complex fabrication processes and increased sources of variability limit both the accessibility and throughput of these models.

Another layer of complexity to some 3D cardiac microtissues is the incorporation of supporting cell types. While some 2D hiPSC-CM cultures contained admixed cell types<sup>90-92</sup>, over 90% of 2D studies used purified hiPSC-CM cultures. In contrast, about half of the 3D hiPSC-CM tissues contained cell types such as mesenchymal stromal cells (SCs) and endothelial cells (ECs) due to either their ability to facilitate tissue compaction or the potential to study the impact of these cell types on cardiac microtissue maturation and function (Fig. 2c). SCs used in these studies include primary cardiac fibroblasts, mesenchymal stem cells, hiPSC-derived cardiac fibroblasts, lung fibroblasts, mural cells, dermal fibroblasts, foreskin fibroblasts, hiPSC-derived stromal cells, hiPSC-derived mural cells, adipose-derived stem cells, pericytes, and hiPSC-derived smooth muscle cells. This variability is consequential, as it has been shown that the stromal cell source can impact tissue assembly and functionality<sup>93</sup>. Additionally, the proportion of stromal cells included, which can impact hiPSC-CM function<sup>94</sup>, varied but many groups either used them in a 1:9 or 1:3 ratio with hiPSC-CMs (Fig. 2d).

Lastly, many groups have also explored the incorporation of ECs to vascularize and further mature cardiac microtissues (Fig. 2c). Not only does vascularization of cardiac microtissues enable the generation of thicker tissues, but the addition of ECs has also been found to mature CMs via paracrine signaling<sup>95</sup>. Prominent EC sources include hiPSC-derived ECs and primary human umbilical vein ECs. In CM-EC-SC tissues, ECs and SCs were most often included in a 1:1 ratio, with over 50% of the tissue being composed of hiPSC-CMs (Fig. 2d).

Overall, the composition of each platform is influenced by the intended use and resource accessibility. This variability in model design can impact the techniques used to assess resulting tissues and their maturation. Dissemination of detailed protocols is critical to making complex cardiac microtissue platforms

widely accessible, allowing others in the field to apply new techniques to improve the maturation and physiological relevance of their models.

### C. Strategies used to mature hiPSC-CMs

Numerous strategies have been developed to simulate developmental cues found in the native cardiac microenvironment to direct hiPSC-CM maturation toward a more adult-like phenotype (Fig. 3). In this analysis, we grouped these cues into five categories (alignment, mechanical, electrical, co-culture, and metabolic maturation techniques) to identify trends in how these techniques are being implemented across the field.

#### *Alignment cues*

Given the high degree of alignment of native cardiomyocytes, alignment cues are common maturation techniques in 2D hiPSC-CM platforms and include micropatterning, aligned electrospun fibrous scaffolds, and grooved surfaces at the microscale<sup>27,53,56,65</sup> and nanoscale<sup>58,61,70</sup> (Fig. 3a). Other variables that may contribute to the success of alignment cues in 2D platforms include adhesive ligand and substrate stiffness. 3D pillar platforms provide alignment via tension, and recent work extended these techniques by bioprinting anisotropic microtissues into larger-scale organized tissue patches<sup>96</sup>.

#### *Mechanical stimulation*

Mechanical maturation techniques include the use of passive tension<sup>96–100</sup>, culturing on hydrogel or elastomeric substrates<sup>66,101,102</sup>, dynamic mechanical stimulation of tissue<sup>83,103–107</sup>, and the application of shear forces<sup>108–110</sup> (Fig. 3a). Across all studies analyzed, mechanical cues were the most used maturation technique (Fig. 3b), likely due to the widespread adoption of 2D hydrogel culture platforms as well as 3D engineered heart tissues (EHTs) composed of tissues tethered between two elastomeric pillars (Fig. 2a-b). Elastic hydrogels of physiologically relevant elastic moduli between 3 to 10 kPa have been shown to improve the maturation and function of hiPSC-CMs compared to supraphysiologic, stiff tissue culture plastic or glass<sup>27,54,102,111</sup>. In EHT platforms, increasing passive tension, or afterload, modulated by pillar stiffness has generally shown to improve tissue formation, CM alignment, and functional maturation<sup>96,112</sup>. However, too high of an afterload can lead to pathological responses<sup>113,114</sup>.

Lastly, cyclic mechanical stimulation to mimic the contractile behavior of the heart and pace hiPSC-CMs in 2D or 3D has been achieved using pressure changes<sup>103,104</sup> and cyclic stretching<sup>105,106,115</sup>. However, this technique was used sparingly, in less than 7% of the studies we analyzed.

#### *Electrical stimulation*

Electrical pacing has shown great improvements in the maturation<sup>116</sup> engineered cardiac microtissue, leading >12% of studies to utilize this technique (Fig. 3b). Previous work showed that initiating electrical stimulation earlier in hiPSC-CM differentiation and gradually increasing stimulation frequency over time (Fig. 3a) can greatly improve the maturation of EHTs compared to the commonly used constant stimulation of 1 Hz initiated later after EHT assembly<sup>116</sup>. These electrically paced tissues had adult-like gene expression profiles, increased mitochondrial density, presence of transverse tubules (t-tubules), and a positive force-frequency relationship.

#### *Co-culture of hiPSC-CMs with other cell types*

As heterocellular signaling plays an important role in native tissue development<sup>24</sup>, there have been significant efforts to characterize the impact of other cell types on hiPSC-CM maturation and overall tissue function. Over 50% of publications incorporated SCs and/or ECs when generating cardiac microtissues (Fig. 2c, 3b), which can improve hiPSC-CM maturation, such as increased formation of t-tubules, contractility, and electrophysiological function<sup>95</sup>. Soluble factors from SCs, without physical co-culture, can also improve the maturation of hiPSC-CMs<sup>117</sup>.

#### *Metabolic maturation*

Strategies focusing on metabolic maturation typically employ media formulations and small molecules that drive a shift from glycolysis to oxidative phosphorylation as the primary source of adenosine triphosphate (ATP) production in hiPSC-CMs. Studies have shown that the use of triiodothyronine<sup>118</sup> and dexamethasone<sup>78</sup> increases mitochondrial activity and improves contractile performance and calcium handling of hiPSC-CMs. Other studies have shown that the switch from media containing glucose to those containing galactose and fatty acids promotes maturation<sup>26,119</sup>. Metabolic maturation is a more nascent technique adopted in under 10% of studies, its ease of implementation makes it likely to be more widely integrated into workflows across labs.

#### *Utilization of maturation techniques*

Despite maturation techniques generally leading to improvements in the function, robustness, and utility of hiPSC-CM models, more than one-third of the studies we analyzed did not use any of these techniques (Fig. 3c). In contrast, many studies combined multiple maturation techniques toward enhancing hiPSC-CM maturation, with about one-third of studies exploring at least two maturation techniques (Fig. 3c). We note a steady increase in the average number of maturation techniques implemented per study from 1.3 in 2016 to 2.0 in 2022 (Fig. 3d). More systematic studies are needed to understand which of these techniques are most successful in driving specific phenotype changes in hiPSC-CMs and how combinations of techniques may act synergistically to improve maturation.

#### **D. Metrics to assess hiPSC-CM maturity and function**

Identifying techniques that are most effective in driving hiPSC-CM maturation requires robust methods to assess hiPSC-CM function. To quantify which assessment metrics are most commonly used and might best inform overall tissue maturity, we examined commonly reported approaches used to obtain data on the structure and function of hiPSC-CMs and derivative tissues.

##### *Structural analyses*

Over 85% of studies reported data on the morphology and organization of sarcomeres in hiPSC-CMs or cardiac microtissues, given the critical role of myofibrils in cell contractile function (Fig. 4a). To obtain these metrics, over 60% of studies performed immunostaining, while over 20% of studies utilized electron microscopy to assess the structure of hiPSC-CMs (Fig. 4b). Proteins that were commonly labeled by immunostaining to visualize hiPSC-CM subcellular structure include cardiac troponin T,  $\alpha$ -actinin, cardiac troponin I,  $\beta$  myosin heavy chain, and connexin-43. While some studies showed qualitative changes, many used immunostaining of sarcomeric proteins to assess myofibril morphometrics, such as sarcomere length and orientation. There are dozens of published image analysis scripts used to analyze sarcomere alignment with unique approaches in sarcomere segmentation and computing gradients, for example<sup>120-124</sup>. These differing methods lead to many metrics of alignment, including orientation order parameter<sup>121,122</sup>, dispersion parameter<sup>124</sup>, and Haralick correlation score<sup>123</sup>, thereby obfuscating direct comparisons across studies.

Methods of imaging the ultrastructure of hiPSC-CMs, mainly focus on identifying key subcellular structural components and their positioning. These features include the relative organization of Z-lines, I-band, H-zones, and M-lines in sarcomeres, the morphology and density of mitochondria, and the presence of caveolae. A structural feature that is associated with high levels of maturation of hiPSC-CMs is the presence and orientation of t-tubules, which has been confirmed in numerous recent studies<sup>31,52,53,78,95,116,125-135</sup>.

##### *Contractility measurements*

Contractility measurements were the second most reported metric of analysis, with over half of the studies reporting a contractility measurement (Fig. 4a). In 2D, the most high-throughput and accessible method of obtaining a contractility metric was using video-based analysis to quantify the displacement of hiPSC-CMs during contraction<sup>27,136</sup>. While this method provides valuable data on contractility kinetics and allows for insight into relative changes in contractility, it does not provide a quantitative value of

contractility that can be compared across studies. A more quantitative contractility metric that is used in 2D is sarcomere shortening, or the fraction that sarcomeres displace relative to their spacing in a relaxed state<sup>121</sup>. While this quantification method can be more readily compared across studies, it still does not directly quantify the contractile force or stress of the cells, and requires live-cell fluorescent labeling of sarcomeres<sup>137</sup>. Traction force microscopy (TFM), in which the displacement of fluorescent beads embedded in an elastic hydrogel is tracked over time, can be used to quantify the contractile force and stress of unpatterned or patterned hiPSC-CMs, both at the single-cell<sup>111</sup> and multicellular<sup>16</sup> level.

Similarly, contractile force and stress of hiPSC-CMs in 3D platforms can be quantified using video-motion analysis of the displacement of tissue constraints of known stiffness such as elastomeric pillars<sup>100</sup>. 3D hiPSC-CM tissues also produce enough force to be captured by force transducers. Among the studies we analyzed that reported contraction metrics, over 15% of studies used force transducers (Fig. 4b)<sup>21,33,135</sup>. To address the variable size of 3D microtissues across and within platforms, contractile stress factoring in tissue geometry should be calculated in addition to force to enable benchmarking of contractility between various platforms. Additionally, we have noted that in traditional EHT systems composed of two elastic pillars that both deflect upon tissue contraction, some groups calculate the EHT contractile force by measuring the displacement of one of the pillars while others other groups sum the deflection of the two pillars to obtain a “total” tissue displacement. However, tension within the suspended tissue is applied equally on each post and thus, the tension in the tissue equals the tension applied at one post, not the sum of the tension at both posts. These observations and suggestions highlight the importance of the quantification method in comparing metrics across studies.

#### *Genetic analyses*

The next most reported metric was gene expression. Most studies that report gene expression used reverse transcription-quantitative polymerase chain reaction (RT-qPCR) to analyze relative changes in expression of genes pre-determined from their study design. A more thorough look at changes in gene expression is now accessible due to many recent innovations in RNA-sequencing, in which the average relative changes in expression of all detected genes can be reported, enabling pathway-level analyses to determine changes in cellular signaling underlying cardiomyocyte maturation.

Genes that were most reported include *MYL2*, *MYH7*, *MYH6*, *TNNT2*, *ATP2A2*, *TNNI3*, *RYR2*, *MYL7*, *GJA1*, *NKX2.5*, *PLN*, *CASQ2*, *SCN5A*, *CACNA1C*, and *KCNJ2* (Fig. 4c). These genes are associated with pathways and proteins involved in cardiac contraction and electrical conduction. As the composition of cardiomyocytes evolves during maturation, their expression of different protein isoforms does as well. Oftentimes, the relative expressions of genes encoding these isoform transitions are reported to assess improvements in maturation (i.e. *MYH7/MYH6*, *MYL2/MYL7*, *TNNI3/TNNI1*).

In addition to gene expression analyses of hiPSC-CM models, over 20% of studies performed other omics analyses. While transcriptomics providing gene expression analyses were the most common, proteomics and metabolomics have also been used recently, often in combination with transcriptomics to better understand transcriptional and translational changes as well as their interrelationship during hiPSC-CM maturation.

#### *Calcium handling and electrophysiological measurements*

Calcium handling and electrophysiological measurements were also common measures of cardiomyocyte function (Fig. 4a), as they are directly related to both the structural and functional maturity of hiPSC-CMs. Calcium handling is most often quantified with calcium sensitive dyes, such as Rhod-2, Fura-2AM, or Fluo-4AM, which enable imaging of calcium dynamics via high-speed microscopy (Fig. 4b). Some studies have also implemented genetically encoded calcium indicators, such as GCaMP<sup>138</sup> to observe calcium transients. Several algorithms have been developed to quantify calcium fluxes<sup>136,139,140</sup>, and cell screening systems have implemented software for the high-throughput analysis of calcium handling.

Similarly, electrophysiology can also be quantified by adding voltage sensitive dyes, such as FluoVolt, Di-4-ANEPPS, Di-8-ANEPPS, or BeRST to CMs, imaging genetically encoded voltage sensors<sup>141</sup>, or by

directly measuring electrical properties using multielectrode arrays (MEA) or patch clamping (Fig. 4b). Patch clamping is the gold standard for electrophysiological recordings of cells, providing specific electrophysiological properties such as resting membrane potential (RMP), that allow for benchmarking of hiPSC-CMs against adult cardiomyocytes. However, it can be difficult to obtain patch clamp measurements from 3D cultures, leading many groups to opt for optical mapping via voltage-sensitive dyes to obtain tissue-scale measurements. One of the most reported metrics from both calcium handling and electrophysiological measurements was conduction velocity, which assesses the maturity of the calcium handling machinery across an entire tissue and the electrical coupling of hiPSC-CMs within the tissue, both of which are critical to the function of myocardial tissue.

#### *Metabolic measurements*

A final metric to report on the maturation of hiPSC-CMs was metabolic activity. As metabolic changes in cardiomyocytes are observed throughout the development of the myocardium, increasing efforts have been made to quantify metabolic activity of hiPSC-CMs to capture the shift from glycolysis to oxidative phosphorylation. Quantifying metabolic activity has become more common in recent years to assess hiPSC-CM maturity, although was still only used by <15% of studies (Fig. 4a).

The most common assay used to quantify metabolic activity was the Agilent Seahorse assay, which monitors ATP production from glycolytic and oxidative pathways in cultures due to changes in free protons and dissolved oxygen in culture medium (Fig. 4b). Of note, <6% of studies provided a measure reflecting the uptake of fatty acids, the main energy source of mature cardiomyocytes<sup>142,143</sup>. Fatty acid uptake was assessed utilizing labeled fatty acids<sup>26,119</sup> or measuring the oxygen consumption rate with the addition of fatty acids<sup>70</sup> and/or a fatty acid oxidation inhibitor<sup>144</sup>. Many of the publications that assess metabolism were also focused on developing methods to specifically mature hiPSC-CMs by directly shifting their metabolic activity<sup>26,119,145,146</sup>, while others used it to assess hiPSC-CM maturation more holistically<sup>95,116,147</sup>.

#### *Response to cardiac modulatory drugs*

A final method for assessing hiPSC-CM maturation was treating cultures with small molecules that are known to impact cardiomyocyte function and quantifying the ability of hiPSC-CMs to respond in a manner reflecting the response of adult cardiomyocytes (Fig. 4d). Most commonly, the beta-adrenergic agonist isoproterenol was added to culture media to quantify the chronotropic and inotropic responses, with a greater contractile force or frequency response indicating increased adrenergic receptors and greater maturity. Other studies utilized small molecules to see if contractility is impaired upon inhibition of specific ion channels found in adult cardiomyocytes and provide insight into the maturity of the calcium handling machinery present<sup>148</sup>.

## **IV. Motivation, progress, and challenges in hiPSC-CM maturity**

### **A. Applications of *in vitro* models requiring improved hiPSC-CM maturity**

#### *Drug screening*

In addition to using drug challenges to assess the maturity of hiPSC-CM tissues, many models show great potential as mid- to high-throughput drug screening platforms. As such, many groups, including regulatory agencies, have begun exploring how patient-specific hiPSC-CM tissues could be used to more accurately identify cardiotoxic effects of therapeutics and ultimately replace expensive and time-consuming *in vivo* cardiotoxicity assays<sup>7</sup>. However, hiPSC-CMs used for cardiotoxicity testing must be sufficiently mature to ensure that the drug-induced phenotype faithfully represents the cardiac response to the drug in human patients.

For example, verapamil can exhibit false positives in commonly used 2D monolayer toxicity assays, prolonging action potential duration at low doses<sup>149</sup>. By treating hiPSC-CMs in 3D culture with maturation media, these effects were no longer observed at relevant doses, likely due to changes in ion channel expression in more mature tissues. This highlights the necessity to generate mature hiPSC-CMs to

accurately assess the potential effectiveness or toxicity of a drug *in vitro*. However, since many studies did not employ maturation techniques, less mature hiPSC-CMs may be sufficient for testing the efficacy and toxicity of certain drugs, depending on their mechanisms of action (Supplementary Data Set 1).

### Disease Modeling

The increased maturation of hiPSC-CM models has also enabled *in vitro* studies of a multitude of cardiac pathologies. Over 15% of the studies analyzed utilized hiPSC-CM platforms to model various cardiac pathologies, ACM, HCM, DCM, myocardial infarction, and long QT syndrome (Fig. 4e,f). By utilizing patient-derived or genetically edited hiPSC-CMs or stress-inducing culture conditions, such as hypoxia, studies have been able to model changes in cardiomyocyte structure, contractility, and electrophysiology associated with pathology<sup>16,21,53,114</sup>. Implementing maturation techniques, such as metabolic conditioning, has enabled the recapitulation of key disease phenotypes that were not otherwise prominent in hiPSC-CMs (Fig. 4f)<sup>21,27,114</sup>. With increasing maturation of hiPSC-CMs, there is growing potential to utilize these models to shed light on disease mechanisms and potential therapeutic approaches.

## B. Field-level improvements in the maturation of hiPSC-CMs

Despite high variability amongst maturation techniques and assessment metrics, there were noticeable improvements in frequently assessed metrics (Fig. 5a-d). Sarcomere length, contractile stress, and conduction velocity all trended upwards over time, suggesting that the field is engineering more mature hiPSC-CMs. Improved measurement tools and techniques could also be contributing to these improvements by enabling more accessible and standardized assessment metrics.

The average reported sarcomere length of hiPSC-CM models increased from ~1.7  $\mu\text{m}$  in 2016-2018 to 1.8-1.9  $\mu\text{m}$  in 2020-2021, approaching the sarcomere length of adult cardiomyocytes, ~2  $\mu\text{m}$ <sup>150</sup> (Fig. 5a). Sarcomere length measurements have been obtained with many different approaches, including the use of different protein markers, imaging techniques, and image analyses. Thus, while maturation strategies should lead to improvements in this value, reported values may also be influenced by the employed measurement methods, each of which may have limitations. While some of the highest reported sarcomere lengths are from hiPSC-CM models from studies exploring maturation techniques such as intensity-ramped electrical stimulation<sup>116</sup>, tri-cultures<sup>151</sup>, or patterned elastomeric substrates<sup>27</sup>, the highest reported average sarcomere length is from a study that did not use any of the maturation techniques assessed here, but instead simply cultured hiPSC-CMs for extended periods of time<sup>129</sup>. Extended culture as a technique for hiPSC-CM maturation has also been explored by other groups, but the use of simplistic, 2D culture platforms employed in these studies appears to limit the development of other features of maturation such as t-tubules<sup>152</sup>.

Contractile stress, on the other hand, has seen more marked improvements in recent years (Fig. 5b). While the average contractile stress of hiPSC-CM models was 12 mN/mm<sup>2</sup> (or 12 kPa) in 2021, more recent models have shown contractile stress performance approaching that of adult cardiomyocytes (25-44 mN/mm<sup>2</sup> or kPa). These models include a micropillar system with passive tension and co-culture<sup>33</sup> and metabolic maturation on micropatterned substrates<sup>21</sup>. While it appears that the use of maturation techniques is important to the improved contractility of hiPSC-CMs, there was no consensus on best techniques.

Numerous maturation strategies have targeted calcium handling and electrophysiology of hiPSC-CMs. As a result, conduction velocity trended upward in recently published work (Fig. 5c). Multiple models achieved average conduction velocities greater than 30 cm/s, including models with dynamic mechanical culture<sup>22</sup>, small molecules targeting signaling pathways<sup>31</sup>, conductive biomaterials<sup>75</sup>, decellularized ECM<sup>153,154</sup>, human perinatal stem cell-derived ECM<sup>40</sup>, ventricular-specific tissues<sup>155</sup>, and 3D printed tri-cultures<sup>156</sup>.

Despite these improvements, resting membrane potential (RMP), another common assessment metric, remained stagnant over time at ~-65 mV with recent decreases towards more adult-like levels (Fig 5d). This could be, at least in part, because many recent advances have been focused on the development of 3D tissues, in which patch-clamp electrophysiology measurements are difficult to obtain directly. Models that have obtained adult-like RMP, below -80 mV, utilized dynamical mechanical stretch<sup>22,114</sup>, ECM-coated

elastomeric surfaces<sup>27,28</sup>, and modifications to culture media<sup>26,30</sup>, all in 2D culture systems. Overall, there is a clear need for improved measurement techniques that accurately assess electrophysiology in 3D tissues.

### C. Variability at all levels of hiPSC-CM tissue formation affects maturation outcomes

A major limitation in the field is difficulty in parsing the individual impacts of each maturation technique due to confounding variables present at all levels of engineering hiPSC-CM tissues. Overall, we found no statistically significant differences in sarcomere length, contractile stress, conduction velocity, and RMP due to the type of maturation technique (Fig. 5f-h). Additionally, utilizing a greater number of maturation techniques did not improve hiPSC-CM performance (Fig. 5i-l). For this analysis, maturation techniques were grouped as described in Figure 3. For instance, tissues formed between elastomeric pillars with stromal cells to aid in compaction would be considered to have utilized two maturation techniques. Thus, while individual studies have shown improvements in hiPSC-CM maturation compared to internal study controls, field-level findings do not reflect this.

Surprisingly, hiPSC-CMs matured with electrical stimulation did not perform as well as hiPSC-CMs matured with other approaches. There are many variables that contribute to differences in electrical stimulation protocols across studies, including the time between differentiation initiation and the beginning of stimulation, stimulation duration, and electrical pulse voltage, width, and frequency. For example, one study showed that constant high-frequency stimulation at 3 Hz leads to mitochondrial dysfunction and increased apoptosis in hiPSC-CMs, while low-frequency stimulation at 1 Hz did not<sup>157</sup>. Another study showed that intensity-ramped frequencies improved the maturation of hiPSC-CMs, likely due to beneficial effects of mimicking the changes in electromechanical loading that occur during the fetal-postnatal transition of cardiomyocytes<sup>116</sup>.

While, it is clear from study-specific experimental controls that maturation techniques exert a positive effect, it is also difficult to parse the individual impacts of each maturation technique because of the numerous variables involved. However, variables at multiple levels prevent comparisons of outcomes across studies and therefore also limit convergence on the most promising maturation strategies.

### V. Collective outlook for improved hiPSC-CM maturation

To begin to rigorously assess progress as a field, we have created an accessible database with the protocol parameters and functional outputs of the 300 studies reported here. These data will allow researchers to determine current trends more easily within the field, directly compare studies, and extract the information needed to replicate a study<sup>34</sup>. We urge researchers to continue to incorporate data from additional publications so that it can stay current and provide a forum for coordinating progress.

The knowledge gained from compiling this database should subsequently be utilized to design comprehensive studies that directly compare current maturation techniques to improve the function and reproducibility of hiPSC-CM models. One way to bypass the influence of protocol variability in determining which maturation techniques are most effective is through a series of studies directly comparing maturation techniques using the same few hiPSC lines within the same platform, culture conditions, measurement techniques, and assessment metrics. This would allow the field to gain a better understanding of which components of the cardiomyocyte are most responsive to a given stimulation, and further, how changes in particular components impact different aspects of cell or cardiac tissue function. Furthermore, measuring the same metrics with the same techniques and software at the same time point is necessary for direct comparisons of hiPSC-CM functionality.

In addition, there are many other parameters that have been understudied as potentially important factors to systematically investigate. For example, there are many different ECM and ECM-like components used in hiPSC-CM models<sup>158</sup>, but there are very few studies investigating the effects of this variable on hiPSC-CM functionality<sup>159,160</sup>. Many protocols across the field are used by only one or a handful of groups and are not systematically compared to other existing protocols. As such, we do not have sufficient data to identify which variables presented yield the best results, which in turn hampers the field from progressing.

To benchmark new approaches against prior literature and future studies, researchers should utilize the same control to report on a predetermined set of metrics. One study directly compared hiPSC-CMs derived from ten different lines and showed wide variability in functional outputs within the same EHT platform<sup>38</sup>. To address this variability, each new study could compare functional properties of hiPSC-CM models to that of the same cell line, perhaps commercially available hiPSC-CMs that come as pre-differentiated CMs, minimizing variability that arises from different differentiation protocols. Experimental techniques, such as maturation media or electrical stimulation, should be tested on hiPSC-CMs in a dish as well as in the engineered platform to separate the effects of experimental techniques from that of the platform on hiPSC-CM maturation. In addition to a shared control line, studies focused on improving hiPSC-CM maturity should utilize at least five hiPSC-CM lines to test the consistency of their protocols. Far more lines should be included when reporting pharmaceutical and therapeutic effects, including a representative number of lines from different sexes and ancestral backgrounds to account for the potential variability in hiPSC-CM responses. There are increasing efforts to establish and share hiPSCs lines from different sexes and ancestral backgrounds<sup>161</sup> that should be further utilized.

While we have highlighted the abundance of metrics used to assess hiPSC-CM structure and function, we propose converging on a few essential metrics that are widely accessible using the same methodology to enable direct comparisons across studies and labs. Some of the most reported metrics that provide important insight into hiPSC-CM maturation include sarcomere/myofibril morphometrics, contractile stress, conduction velocity, and gene expression. Some metrics are highly sensitive to the specific image analysis pipeline utilized. Thus, it would be critical to develop and jointly adopt open-source analysis pipelines that robustly handle data generated from a range of different platforms to enable direct comparison of data across experiments and labs. Further, we encourage the use of voltage-sensitive dyes, such as FluoVolt or Di-4-ANEPPS, or calcium-sensitive dyes, such as Fluo-4AM, to report conduction velocity<sup>162</sup>. Additionally, hiPSC-CMs should be electrically paced during calcium handling analysis to reduce variability in calcium handling metrics resulting from inconsistent spontaneous contractions of immature hiPSC-CMs. Lastly, gene expression ratios of key maturation-related genes, such as *MYH7/MYH6*, *MYL2/MYL7*, and *TNNI3/TNNI1*, should be reported.

Implementing common analysis software and experimental controls in future experiments, and subsequently updating our database with these new results, will facilitate the growth of a resource that can be mined using machine learning and high-dimensional data analysis techniques. Analyzing a more comprehensive dataset using such techniques could glean valuable insights into the effects of specific maturation techniques or combinations thereof on maturation outcomes. While the current dataset presented here is currently the most comprehensive analysis in this space, the lack of consistency among studies and limited number of comparable datapoints makes such analyses quite challenging. As such, once a more comprehensive dataset can be compiled, these techniques and others could be leveraged to extract information that can guide continued progress of the field toward generating mature hiPSC-CMs and derivative cardiac tissue.

While we focus on *in vitro* hiPSC-CM models, much of the insights from this analysis can be used to inform *in vivo* implantation of hiPSC-CM-based tissue patches or cardiac regeneration studies using animal models<sup>22–24</sup>. Delivery and implantation of hiPSC-CMs *in vivo* has made great progress, showing improved function in the injured heart<sup>22,23</sup>, however, this introduces additional variables and complex outputs to assess, such as host integration and system-wide functional changes. Similar comprehensive benchmarking of the potential variables inherent to these complex experiments, like the analysis conducted on *in vitro* hiPSC-CM systems presented here, is necessary and would greatly move the field forward. Additionally, while *in vitro* tissue platforms have great potential to model disease and expedite the drug discovery process, synergizing findings from these platforms with animal models or patient samples is critical towards gaining a comprehensive understanding of cardiac pathophysiology. More specifically, it may be necessary to verify findings from reductionist *in vitro* models in more complex *in vivo* settings before moving forward with specific disease modeling studies, for example. Additionally, due to their increased complexity, various animal models can provide unique insights into specific processes involved important in cardiac development, regeneration and disease progression and thus should be used to inform the design of novel *in vitro* models.

The multidisciplinary nature of the cardiac tissue engineering field brings together clinicians, biologists, and engineers. Providing researchers from diverse perspectives with a standardized venue to report their findings will allow them to learn from each other and move forward more efficiently. These types of analyses will allow the field to streamline advances in developing models for drug discovery and therapies for cardiac pathologies.

## VI. Conclusion

In recent years, there has been significant progress in the field of cardiac tissue engineering toward generating mature tissues composed of hiPSC-CMs for use as disease models and drug screening platforms. However, quantitatively benchmarking progress across the field has proved challenging due to variability in many aspects of tissue formation, culture, and subsequent assessment, including the choice of hiPSC lines, differentiation protocols for generating CMs, platforms for forming tissues, maturation techniques, and various measurements used to assess cell or tissue function. Given the many sources of variability at multiple levels, it is difficult to ascertain which techniques are most effective in improving the maturation of hiPSC-CMs or derivative tissues formed from these cells. Here, we highlight the need for convergence on controls and quantitative analysis methods that will enable more efficient progress toward generating hiPSC-CM tissues that recapitulate adult cardiac physiology with utility for numerous applications. Further, we have made all data used in this analysis freely accessible and encourage others in the field to contribute to and utilize this database to better inform their ongoing research and support the collective advancement of the field as a whole<sup>34</sup>.

## Data Availability Statement

The data supporting the findings of this field-wide analysis are available within the manuscript and Supporting Information. Additionally, the data set has been deposited on Dryad and will continue to be updated as new manuscripts are published in this area of research (<https://doi.org/10.5061/dryad.ksn02v7bh>)<sup>34</sup>.

## Acknowledgements

This work was funded by the National Science Foundation (NSF) Engineering Research Center on Cellular Metamaterials (EEC-1647837). J.K.E acknowledges financial support from the National Institute of Health National Heart, Lung, and Blood (F31 HL158195-03). S.J.D. and B.M.B. acknowledge financial support from the NSF (2033654). S.J.D. acknowledges support from the National Institute of Health (T32-DE007057 and T32-HL125242). J.K.E. and X.G. acknowledge funding support from the NSF Graduate Research Fellowship Program. L.L. acknowledges support provided by the Florida Heart Research Foundation. C.S.C. acknowledges support from NSF (CMMI-1548571 and DGE-2244366) and the Paul G. Allen Frontiers Group Allen Distinguished Investigator Program.

## Author Contributions

J.K.E. and S.J.D. contributed equally, led and performed analysis, wrote and reviewed the manuscript. B.M.B. and C.S.C. jointly supervised this work, wrote, and reviewed the manuscript. M.E.J., M.C.K., Y-M.L., P.M., X.G., L.L., M.M., J.T., M.A.M., A.C.S.C. performed analysis and reviewed the manuscript. J.H., K.C.T. Jr., T.G.B., S.R., A.E.W., A.A. E.L supervised analysis and reviewed the manuscript.

## Ethics Declaration

C.S.C. is a founder and owns shares of Satellite Biosciences, a company that is developing cell-based therapies. All other authors declare no competing interests.

## References

1. Wouters, O. J., McKee, M. & Luyten, J. Estimated Research and Development Investment Needed to Bring a New Medicine to Market, 2009-2018. *JAMA* **323**, 844–853 (2020).

2. Varga, Z. V., Ferdinand, P., Liaudet, L. & Pacher, P. Drug-induced mitochondrial dysfunction and cardiotoxicity. *American Journal of Physiology - Heart and Circulatory Physiology* **309**, H1453–H1467 (2015).
3. Bird, S. D. *et al.* The human adult cardiomyocyte phenotype. *Cardiovasc Res* **58**, 423–434 (2003).
4. Milani-Nejad, N. & Janssen, P. M. L. Small and large animal models in cardiac contraction research: Advantages and disadvantages. *Pharmacology and Therapeutics* **14**, 235–249 (2014).
5. Maltsev, V. A., Rohwedel, J., Hescheler, J. & Wobus, A. M. Embryonic Stem Cells Differentiate in Vitro into Cardiomyocytes Representing Sinusnodal, Atrial and Ventricular Cell Types. *Mechanisms of Development* **44**, 41-50 (1993).
6. Takahashi, K. *et al.* Induction of Pluripotent Stem Cells from Adult Human Fibroblasts by Defined Factors. *Cell* **131**, 861–872 (2007).
7. Colatsky, T. *et al.* The Comprehensive in Vitro Proarrhythmia Assay (CiPA) initiative — Update on progress. *J Pharmacol Toxicol Methods* **81**, 15–20 (2016).
8. McKenna, W. J. & Judge, D. P. Epidemiology of the inherited cardiomyopathies. *Nature Reviews Cardiology* **18**, 22–36 (2021).
9. Ho, C. Y. *et al.* Genotype and lifetime burden of disease in hypertrophic cardiomyopathy insights from the sarcomeric human cardiomyopathy registry (SHaRe). *Circulation* **138**, 1387–1398 (2018).
10. Lippi, M. *et al.* Spectrum of Rare and Common Genetic Variants in Arrhythmogenic Cardiomyopathy Patients. *Biomolecules* **12**, 1043 (2022).
11. Haas, J. *et al.* Atlas of the clinical genetics of human dilated cardiomyopathy. *European Heart Journal* **36**, 1123–1135 (2015).
12. Bhagwan, J. R. *et al.* Isogenic models of hypertrophic cardiomyopathy unveil differential phenotypes and mechanism-driven therapeutics. *J Mol Cell Cardiol* **145**, 43–53 (2020).
13. Mosqueira, D. *et al.* CRISPR/Cas9 editing in human pluripotent stemcell-cardiomyocytes highlights arrhythmias, hypocontractility, and energy depletion as potential therapeutic targets for hypertrophic cardiomyopathy. *Eur Heart J* **39**, 3879–3892 (2018).
14. Loiben, A. M. *et al.* Cardiomyocyte Apoptosis Is Associated with Contractile Dysfunction in Stem Cell Model of MYH7 E848G Hypertrophic Cardiomyopathy. *Int J Mol Sci* **24**, (2023).
15. Prondzynski, M. *et al.* Disease modeling of a mutation in  $\alpha$ -actinin 2 guides clinical therapy in hypertrophic cardiomyopathy. *EMBO Mol Med* **11**, (2019).
16. Zhang, K. *et al.* Plakophilin-2 Truncating Variants Impair Cardiac Contractility by Disrupting Sarcomere Stability and Organization. *Sci. Adv* **7**, (2021).
17. Cohn, R. *et al.* A Contraction Stress Model of Hypertrophic Cardiomyopathy due to Sarcomere Mutations. *Stem Cell Reports* **12**, 71–83 (2019).
18. Hinson, J. T. *et al.* Titin Mutations in IPS Cells Define Sarcomere Insufficiency as a Cause of Dilated Cardiomyopathy **349**, (2015).
19. Toepfer, C. N. *et al.* Myosin Sequestration Regulates Sarcomere Function, Cardiomyocyte Energetics, and Metabolism, Informing the Pathogenesis of Hypertrophic Cardiomyopathy. *Circulation* 828–842 (2020).
20. Briganti, F. *et al.* iPSC Modeling of RBM20-Deficient DCM Identifies Upregulation of RBM20 as a Therapeutic Strategy. *Cell Rep* **32**, (2020).
21. Knight, W. E. *et al.* Maturation of Pluripotent Stem Cell-Derived Cardiomyocytes Enables Modeling of Human Hypertrophic Cardiomyopathy. *Stem Cell Reports* **16**, 519–533 (2021). An informative study utilizing a combination of metabolic maturation and micropatterned surfaces to improve the maturation of hiPSC-CMs, increasing sensitivity to pathological stimuli.
22. Querdel, E. *et al.* Human Engineered Heart Tissue Patches Remuscularize the Injured Heart in a Dose-Dependent Manner. *Circulation* **143**, 1991–2006 (2021). An informative study utilizing dynamic mechanical stimulation of engineered heart tissue patches to obtain improved maturation of hiPSC-CMs. Transplantation of the patches resulted in partial remuscularization of the injured heart in a guinea pig injury model.

23. Liu, Y. W. *et al.* Human embryonic stem cell-derived cardiomyocytes restore function in infarcted hearts of non-human primates. *Nat Biotechnol* **36**, 597–605 (2018).
24. Karbassi, E. *et al.* Cardiomyocyte maturation: advances in knowledge and implications for regenerative medicine. *Nature Reviews Cardiology* **17**, 341–359 (2020). A comprehensive review on the structural and functional characteristics of mature cardiomyocytes.
25. Yang, X., Pabon, L. & Murry, C. E. Engineering adolescence: Maturation of human pluripotent stem cell-derived cardiomyocytes. *Circulation Research* **114**, 511–523 (2014).
26. Feyen, D. A. M. *et al.* Metabolic Maturation Media Improve Physiological Function of Human iPSC-Derived Cardiomyocytes. *Cell Rep* **32**, (2020). An informative study utilizing metabolic maturation techniques in 2D and 3D, obtaining improved functional maturation of hiPSC-CMs.
27. Tsan, Y. C. *et al.* Physiologic biomechanics enhance reproducible contractile development in a stem cell derived cardiac muscle platform. *Nat Commun* **12**, (2021). An informative study utilizing micropatterning on elastomer substrates to define tissue biomechanics and improve the maturation of hiPSC-CMs.
28. Herron, T. J. *et al.* Extracellular matrix-mediated maturation of human pluripotent stem cell-derived cardiac monolayer structure and electrophysiological function. *Circ Arrhythm Electrophysiol* **9**, (2016).
29. Martella, D. *et al.* Liquid Crystalline Networks toward Regenerative Medicine and Tissue Repair. *Small* **13**, (2017).
30. Lin, B. *et al.* Culture in glucose-depleted medium supplemented with fatty acid and 3,3',5-Triiodo-L-thyronine facilitates purification and maturation of human pluripotent stem cell-derived cardiomyocytes. *Front Endocrinol* **8**, (2017).
31. Miki, K. *et al.* ERR $\gamma$  enhances cardiac maturation with T-tubule formation in human iPSC-derived cardiomyocytes. *Nat Commun* **12**, (2021).
32. Mulieri, L. A., Hasenfuss, G., Leavitt, B., Allen, P. D. & Alpert, N. R. Altered Myocardial Force-Frequency Relation in Human Heart Failure. *Circulation* **85**, 1743–1750 (1992).
33. Melby, J. A. *et al.* Functionally Integrated Top-Down Proteomics for Standardized Assessment of Human Induced Pluripotent Stem Cell-Derived Engineered Cardiac Tissues. *J Proteome Res* **20**, 1424–1433 (2021). An informative study establishing a method allowing for the sequential assessment of functional properties and top-down proteomics for hiPSC-engineered cardiac tissue.
34. Ewoldt, J. K. and DePalma, S. J. *et al.* Induced pluripotent stem cell-derived cardiomyocyte in vitro models: tissue fabrication protocols, assessment methods, and quantitative maturation metrics for benchmarking progress [Dataset]. *Dryad* (2023).
35. Lapp, H. *et al.* Author Correction: Frequency-dependent drug screening using optogenetic stimulation of human iPSC-derived cardiomyocytes. *Scientific Reports* **11**, (2021).
36. Schnabel, L. V., Abratte, C. M., Schimenti, J. C., Southard, T. L. & Fortier, L. A. Genetic background affects induced pluripotent stem cell generation. *Stem Cell Res Ther* **3**, (2012).
37. Rouhani, F. *et al.* Genetic Background Drives Transcriptional Variation in Human Induced Pluripotent Stem Cells. *PLoS Genet* **10**, (2014).
38. Mannhardt, I. *et al.* Comparison of 10 Control hPSC Lines for Drug Screening in an Engineered Heart Tissue Format. *Stem Cell Reports* **15**, 983–998 (2020). An informative study comparing 10 different control hiPSC-CM lines in engineered heart tissue to demonstrate large baseline cell-line dependent differences in tissue function.
39. Marinho, P. A., Chailangkarn, T. & Muotri, A. R. Systematic optimization of human pluripotent stem cells media using Design of Experiments. *Sci Rep* **5**, (2015).
40. Block, T. *et al.* Human perinatal stem cell derived extracellular matrix enables rapid maturation of hiPSC-CM structural and functional phenotypes. *Sci Rep* **10**, (2020).
41. Zhang, J. *et al.* Cardiac differentiation of human pluripotent stem cells using defined extracellular matrix proteins reveals essential role of fibronectin. *Elife* **11**, (2022).
42. Lian, X. *et al.* Robust cardiomyocyte differentiation from human pluripotent stem cells via temporal modulation of canonical Wnt signaling. *Proc Natl Acad Sci U S A* **109**, (2012).

43. Mummery, C. L. *et al.* Differentiation of human embryonic stem cells and induced pluripotent stem cells to cardiomyocytes: A methods overview. *Circulation Research* **111**, 344–358 (2012).

44. Tohyama, S. *et al.* Distinct Metabolic Flow Enables Large-Scale Purification of Mouse and Human Pluripotent Stem Cell-Derived Cardiomyocytes. *Cell Stem Cell* **12**, 127–137 (2013).

45. Xu, C. *et al.* Bioinspired onion epithelium-like structure promotes the maturation of cardiomyocytes derived from human pluripotent stem cells. *Biomater Sci* **5**, 1810–1819 (2017).

46. Ma, Z. *et al.* Self-organizing human cardiac microchambers mediated by geometric confinement. *Nat Commun* **6**, (2015).

47. Schulz, A. *et al.* Tyramine-conjugated alginate hydrogels as a platform for bioactive scaffolds. *J Biomed Mater Res A* **107**, 114–121 (2019).

48. Hart, C. *et al.* Rapid nanofabrication of nanostructured interdigitated electrodes (NIDES) for long-term in vitro analysis of human induced pluripotent stem cell differentiated cardiomyocytes. *Biosensors* **8**, (2018).

49. Sun, S. *et al.* Progressive Myofibril Reorganization of Human Cardiomyocytes on a Dynamic Nanotopographic Substrate. *ACS Appl Mater Interfaces* **12**, 21450–21462 (2020).

50. Martewicz, S. *et al.* Transcriptomic Characterization of a Human In Vitro Model of Arrhythmogenic Cardiomyopathy Under Topological and Mechanical Stimuli. *Ann Biomed Eng* **47**, 852–865 (2019).

51. Kujala, V. J., Pasqualini, F. S., Goss, J. A., Nawroth, J. C. & Parker, K. K. Laminar ventricular myocardium on a microelectrode array-based chip. *J Mater Chem B* **4**, 3534–3543 (2016).

52. Pioner, J. M. *et al.* Isolation and mechanical measurements of myofibrils from human induced pluripotent stem cell-derived cardiomyocytes. *Stem Cell Reports* **6**, 885–896 (2016).

53. Strimaityte, D. *et al.* Contractility and Calcium Transient Maturation in the Human iPSC-Derived Cardiac Microfibers. *ACS Appl Mater Interfaces* **14**, 35376–35388 (2022).

54. Wheelwright, M. *et al.* Investigation of human iPSC-derived cardiac myocyte functional maturation by single cell traction force microscopy. *PLoS One* **13**, (2018).

55. Kit-Anan, W. *et al.* Multiplexing physical stimulation on single human induced pluripotent stem cell-derived cardiomyocytes for phenotype modulation. *Biofabrication* **13**, (2021).

56. Wanjare, M. *et al.* Anisotropic microfibrous scaffolds enhance the organization and function of cardiomyocytes derived from induced pluripotent stem cells. *Biomater Sci* **5**, 1567–1578 (2017).

57. Kumar, N. *et al.* Scalable Biomimetic Coaxial Aligned Nanofiber Cardiac Patch: A Potential Model for “Clinical Trials in a Dish”. *Front Bioeng Biotechnol* **8**, (2020).

58. Depalma, S. J., Davidson, C. D., Stis, A. E., Helms, A. S. & Baker, B. M. Microenvironmental determinants of organized iPSC-cardiomyocyte tissues on synthetic fibrous matrices. *Biomater Sci* **9**, 93–107 (2021).

59. Li, J. *et al.* Extracellular recordings of patterned human pluripotent stem cell-derived cardiomyocytes on aligned fibers. *Stem Cells Int* **2016**, (2016).

60. Chun, Y. W. *et al.* Combinatorial polymer matrices enhance in vitro maturation of human induced pluripotent stem cell-derived cardiomyocytes. *Biomaterials* **67**, 52–64 (2015).

61. Khan, M. *et al.* Evaluation of changes in morphology and function of human induced pluripotent stem cell derived cardiomyocytes (hiPSC-CMs) cultured on an aligned-nanofiber cardiac patch. *PLoS One* **10**, (2015).

62. Pushp, P. *et al.* Functional comparison of beating cardiomyocytes differentiated from umbilical cord-derived mesenchymal/stromal stem cells and human foreskin-derived induced pluripotent stem cells. *J Biomed Mater Res A* **108**, 496–514 (2020).

63. Chen, Y., Chan, J. P. Y., Wu, J., Li, R. K. & Santerre, J. P. Compatibility and function of human induced pluripotent stem cell derived cardiomyocytes on an electrospun nanofibrous scaffold, generated from an ionomeric polyurethane composite. *J Biomed Mater Res A* **110**, 1932–1943 (2022).

64. Tang, Y. *et al.* Induction and differentiation of human induced pluripotent stem cells into functional cardiomyocytes on a compartmented monolayer of gelatin nanofibers. *Nanoscale* **8**, 14530–14540 (2016).

65. Takada, T. *et al.* Aligned human induced pluripotent stem cell-derived cardiac tissue improves contractile properties through promoting unidirectional and synchronous cardiomyocyte contraction. *Biomaterials* **281**, (2022).

66. Pioneer, J. M. *et al.* Optical investigation of action potential and calcium handling maturation of hiPSC-cardiomyocytes on biomimetic substrates. *Int J Mol Sci* **20**, (2019).

67. Huethorst, E. *et al.* Customizable, engineered substrates for rapid screening of cellular cues. *Biofabrication* **12**, (2020).

68. Carson, D. *et al.* Nanotopography-Induced Structural Anisotropy and Sarcomere Development in Human Cardiomyocytes Derived from Induced Pluripotent Stem Cells. *ACS Applied Materials and Interfaces* **8**, 21923–21932 (2016).

69. Smith, A. S. T. *et al.* NanoMEA: A Tool for High-Throughput, Electrophysiological Phenotyping of Patterned Excitable Cells. *Nano Lett* **20**, 1561–1570 (2020).

70. Afzal, J. *et al.* Cardiac ultrastructure inspired matrix induces advanced metabolic and functional maturation of differentiated human cardiomyocytes. *Cell Rep* **40**, (2022).

71. Cui, H. *et al.* 4D Physiologically Adaptable Cardiac Patch: A 4-Month in Vivo Study for the Treatment of Myocardial Infarction. *Sci Adv* **6**, (2020).

72. Zhang, Y. S. *et al.* Bioprinting 3D microfibrous scaffolds for engineering endothelialized myocardium and heart-on-a-chip. *Biomaterials* **110**, 45–59 (2016).

73. Gao, L. *et al.* Myocardial Tissue Engineering with Cells Derived from Human-Induced Pluripotent Stem Cells and a Native-Like, High-Resolution, 3-Dimensionally Printed Scaffold. *Circ Res* **120**, 1318–1325 (2017).

74. Feaster, T. K., Casciola, M., Narkar, A. & Blinova, K. Acute effects of cardiac contractility modulation on human induced pluripotent stem cell-derived cardiomyocytes. *Physiol Rep* **9**, (2021).

75. Lind, J. U. *et al.* Instrumented cardiac microphysiological devices via multimaterial three-dimensional printing. *Nat Mater* **16**, 303–308 (2017).

76. Jia, J. *et al.* Development of peptide-functionalized synthetic hydrogel microarrays for stem cell and tissue engineering applications. *Acta Biomater* **45**, 110–120 (2016).

77. Park, S. J. *et al.* Insights into the Pathogenesis of Catecholaminergic Polymorphic Ventricular Tachycardia from Engineered Human Heart Tissue. *Circulation* **140**, 390–404 (2019).

78. Parikh, S. S. *et al.* Thyroid and Glucocorticoid Hormones Promote Functional T-Tubule Development in Human-Induced Pluripotent Stem Cell-Derived Cardiomyocytes. *Circ Res* **121**, 1323–1330 (2017).

79. Garbern, J. C. *et al.* Inhibition of mTOR Signaling Enhances Maturation of Cardiomyocytes Derived from Human-Induced Pluripotent Stem Cells via p53-Induced Quiescence. *Circulation* **285–300** (2020).

80. Pasqualini, F. S., Sheehy, S. P., Agarwal, A., Aratyn-Schaus, Y. & Parker, K. K. Structural phenotyping of stem cell-derived cardiomyocytes. *Stem Cell Reports* **4**, 340–347 (2015).

81. Buikema, J. W. *et al.* Wnt Activation and Reduced Cell-Cell Contact Synergistically Induce Massive Expansion of Functional Human iPSC-Derived Cardiomyocytes. *Cell Stem Cell* **27**, 50–63 (2020).

82. Guo, J. *et al.* Elastomer-grafted iPSC-derived micro heart muscles to investigate effects of mechanical loading on physiology. *ACS Biomater Sci Eng* **7**, 2973–2989 (2021).

83. Dou, W. *et al.* A microdevice platform for characterizing the effect of mechanical strain magnitudes on the maturation of iPSC-Cardiomyocytes. *Biosens Bioelectron* **175**, (2021).

84. Kroll, K. *et al.* Electro-mechanical conditioning of human iPSC-derived cardiomyocytes for translational research. *Prog Biophys Mol Biol* **130**, 212–222 (2017).

85. Noor, N. *et al.* 3D Printing of Personalized Thick and Perfusionable Cardiac Patches and Hearts. *Advanced Science* **6**, (2019).

86. Schwan, J. *et al.* Anisotropic engineered heart tissue made from laser-cut decellularized myocardium. *Sci Rep* **6**, (2016).

87. Goldfracht, I. *et al.* Engineered heart tissue models from hiPSC-derived cardiomyocytes and cardiac ECM for disease modeling and drug testing applications. *Acta Biomater* **92**, 145–159 (2019).

88. Blazeski, A. *et al.* Functional Properties of Engineered Heart Slices Incorporating Human Induced Pluripotent Stem Cell-Derived Cardiomyocytes. *Stem Cell Reports* **12**, 982–995 (2019).

89. Vannozzi, L. *et al.* Self-Folded Hydrogel Tubes for Implantable Muscular Tissue Scaffolds. *Macromol Biosci* **18**, (2018).

90. Abecasis, B. *et al.* Unveiling the molecular crosstalk in a human induced pluripotent stem cell-derived cardiac model. *Biotechnol Bioeng* **116**, 1245–1252 (2019).

91. Floy, M. E. *et al.* Direct coculture of human pluripotent stem cell-derived cardiac progenitor cells with epicardial cells induces cardiomyocyte proliferation and reduces sarcomere organization. *J Mol Cell Cardiol* **162**, 144–157 (2022).

92. Peters, M. C. *et al.* Follistatin-like 1 promotes proliferation of matured human hypoxic iPSC-cardiomyocytes and is secreted by cardiac fibroblasts. *Mol Ther Methods Clin Dev* **25**, 3–16 (2022).

93. Hookway, T. A. *et al.* Phenotypic Variation between Stromal Cells Differentially Impacts Engineered Cardiac Tissue Function. *Tissue Eng Part A* **25**, 773–785 (2019).

94. Rupert, C. E., Kim, T. Y., Choi, B. R. & Coulombe, K. L. K. Human Cardiac Fibroblast Number and Activation State Modulate Electromechanical Function of hiPSC-Cardiomyocytes in Engineered Myocardium. *Stem Cells Int* **2020**, (2020).

95. Giacomelli, E. *et al.* Human-iPSC-Derived Cardiac Stromal Cells Enhance Maturation in 3D Cardiac Microtissues and Reveal Non-cardiomyocyte Contributions to Heart Disease. *Cell Stem Cell* **26**, 862–879 (2020). An informative study parsing the impact of co-culture with cardiac fibroblasts and endothelial cells on the maturation of hiPSC-CMs in scaffold-free cardiac spheroids.

96. Ahrens, J. H. *et al.* Programming Cellular Alignment in Engineered Cardiac Tissue via Bioprinting Anisotropic Organ Building Blocks. *Advanced Materials* **34**, (2022).

97. Feric, N. T. *et al.* Engineered Cardiac Tissues Generated in the Biowire II: A Platform for Human-Based Drug Discovery. *Toxicological Sciences* **172**, 89–97 (2019).

98. Tamargo, M. A. *et al.* MilliPillar: A Platform for the Generation and Real-Time Assessment of Human Engineered Cardiac Tissues. *ACS Biomater Sci Eng* **7**, 5215–5229 (2021).

99. Ulmer, B. M. *et al.* Contractile Work Contributes to Maturation of Energy Metabolism in hiPSC-Derived Cardiomyocytes. *Stem Cell Reports* **10**, 834–847 (2018).

100. Boudou, T. *et al.* A microfabricated platform to measure and manipulate the mechanics of engineered cardiac microtissues. *Tissue Eng Part A* **18**, 910–919 (2012).

101. Lee, S. *et al.* Contractile force generation by 3D hiPSC-derived cardiac tissues is enhanced by rapid establishment of cellular interconnection in matrix with muscle-mimicking stiffness. *Biomaterials* **131**, 111–120 (2017).

102. Feaster, T. K. *et al.* A method for the generation of single contracting human-induced pluripotent stem cell-derived cardiomyocytes. *Circ Res* **117**, 995–1000 (2015).

103. Jayne, R. K. *et al.* Direct laser writing for cardiac tissue engineering: A microfluidic heart on a chip with integrated transducers. *Lab Chip* **21**, 1724–1737 (2021).

104. Rogers, A. J., Fast, V. G. & Sethu, P. Biomimetic Cardiac Tissue Model Enables the Adaption of Human Induced Pluripotent Stem Cell Cardiomyocytes to Physiological Hemodynamic Loads. *Anal Chem* **88**, 9862–9868 (2016).

105. Ng, R. *et al.* Contractile work directly modulates mitochondrial protein levels in human engineered heart tissues. *Am J Physiol Heart Circ Physiol* **318**, 1516–1524 (2020).

106. Ma, X. *et al.* 3D printed micro-scale force gauge arrays to improve human cardiac tissue maturation and enable high throughput drug testing. *Acta Biomater* **95**, 319–327 (2019).

107. Ruan, J. L. *et al.* Mechanical stress promotes maturation of human myocardium from pluripotent stem cell-derived progenitors. *Stem Cells* **33**, 2148–2157 (2015).

108. Kolanowski, T. J. *et al.* Enhanced structural maturation of human induced pluripotent stem cell-derived cardiomyocytes under a controlled microenvironment in a microfluidic system. *Acta Biomater* **102**, 273–286 (2020).

109. Marsano, A. *et al.* Beating heart on a chip: A novel microfluidic platform to generate functional 3D cardiac microtissues. *Lab Chip* **16**, 599–610 (2016).

110. Gao, L. *et al.* Large cardiac muscle patches engineered from human induced-pluripotent stem cell-derived cardiac cells improve recovery from myocardial infarction in swine. *Circulation* **137**, 1712–1730 (2018).

111. Ribeiro, A. J. S. *et al.* Contractility of Single cardiomyocytes differentiated from pluripotent stem cells depends on physiological shape and substrate stiffness. *Proc Natl Acad Sci U S A* **112**, 12705–12710 (2015).

112. Abilez, O. J. *et al.* Passive Stretch Induces Structural and Functional Maturation of Engineered Heart Muscle as Predicted by Computational Modeling. *Stem Cells* **36**, 265–277 (2018).

113. Leonard, A. *et al.* Afterload promotes maturation of human induced pluripotent stem cell derived cardiomyocytes in engineered heart tissues. *J Mol Cell Cardiol* **118**, 147–158 (2018).

114. Bliley, J. M. *et al.* Dynamic loading of human engineered heart tissue enhances contractile function and drives a desmosome-linked disease phenotype. *Sci. Transl. Med* **13**, 1817 (2021).

115. Ruan, J. L. *et al.* Mechanical Stress Conditioning and Electrical Stimulation Promote Contractility and Force Maturation of Induced Pluripotent Stem Cell-Derived Human Cardiac Tissue. *Circulation* **134**, 1557–1567 (2016).

116. Ronaldson-Bouchard, K. *et al.* Advanced maturation of human cardiac tissue grown from pluripotent stem cells. *Nature* **556**, 239–243 (2018). An informative study demonstrating the effectiveness of electromechanical training for the maturation of hiPSC-CMs.

117. Yoshida, S. *et al.* Maturation of Human Induced Pluripotent Stem Cell-Derived Cardiomyocytes by Soluble Factors from Human Mesenchymal Stem Cells. *Molecular Therapy* **26**, 2681–2695 (2018).

118. Yang, X. *et al.* Tri-iodo-l-thyronine promotes the maturation of human cardiomyocytes-derived from induced pluripotent stem cells. *J Mol Cell Cardiol* **72**, 296–304 (2014).

119. Correia, C. *et al.* Distinct carbon sources affect structural and functional maturation of cardiomyocytes derived from human pluripotent stem cells. *Sci Rep* **7**, (2017). An informative study demonstrating the link between metabolic substrate utilization and functional maturation of hiPSC-CMs.

120. Zhao, B., Zhang, K., Chen, C. S. & Lejeune, E. Sarc-Graph: Automated segmentation, tracking, and analysis of sarcomeres in hiPSCderived cardiomyocytes. *PLoS Comput Biol* **17**, (2021).

121. Toepfer, C. N. *et al.* SarcTrack. *Circ Res* **124**, 1172–1183 (2019).

122. Morrill, E. E. *et al.* A validated software application to measure fiber organization in soft tissue. *Biomech Model Mechanobiol* **15**, 1467–1478 (2016).

123. Stein, J. M. *et al.* Software Tool for Automatic Quantification of Sarcomere Length and Organization in Fixed and Live 2D and 3D Muscle Cell Cultures In Vitro. *Curr Protoc* **2**, (2022).

124. Sutcliffe, M. D. *et al.* High content analysis identifies unique morphological features of reprogrammed cardiomyocytes. *Sci Rep* **8**, (2018).

125. Mills, R. J. *et al.* Functional screening in human cardiac organoids reveals a metabolic mechanism for cardiomyocyte cell cycle arrest. *Proc Natl Acad Sci U S A* **114**, E8372–E8381 (2017).

126. Fukushima, H. *et al.* Specific induction and long-term maintenance of high purity ventricular cardiomyocytes from human induced pluripotent stem cells. *PLoS One* **15**, (2020).

127. Garay, B. I. *et al.* Dual inhibition of MAPK and PI3K/AKT pathways enhances maturation of human iPSC-derived cardiomyocytes. *Stem Cell Reports* **17**, 2005–2022 (2022).

128. Ergir, E. *et al.* Generation and maturation of human iPSC-derived 3D organotypic cardiac microtissues in long-term culture. *Sci Rep* **12**, (2022).

129. Cui, N. *et al.* Doxorubicin-induced cardiotoxicity is maturation dependent due to the shift from topoisomerase II $\alpha$  to II $\beta$  in human stem cell derived cardiomyocytes. *J Cell Mol Med* **23**, 4627–4639 (2019).

130. Jabbour, R. J. *et al.* In vivo grafting of large engineered heart tissue patches for cardiac repair. (2021) doi:10.1172/jci.

131. Hatani, T. *et al.* Nano-structural analysis of engrafted human induced pluripotent stem cell-derived cardiomyocytes in mouse hearts using a genetic-probe APEX2. *Biochem Biophys Res Commun* **505**, 1251–1256 (2018).

132. Kerscher, P. *et al.* Direct hydrogel encapsulation of pluripotent stem cells enables ontomimetic differentiation and growth of engineered human heart tissues. *Biomaterials* **83**, 383–395 (2016).

133. Huang, C. Y. *et al.* Enhancement of human iPSC-derived cardiomyocyte maturation by chemical conditioning in a 3D environment. *J Mol Cell Cardiol* **138**, 1–11 (2020).

134. Mannhardt, I. *et al.* Human Engineered Heart Tissue: Analysis of Contractile Force. *Stem Cell Reports* **7**, 29–42 (2016).

135. Shadrin, I. Y. *et al.* Cardiopatch platform enables maturation and scale-up of human pluripotent stem cell-derived engineered heart tissues. *Nat Commun* **8**, (2017).

136. Huebsch, N. *et al.* Automated video-based analysis of contractility and calcium flux in human-induced pluripotent stem cell-derived cardiomyocytes cultured over different spatial scales. *Tissue Eng Part C Methods* **21**, 467–479 (2015).

137. Sharma, A., Toepfer, C. N., Schmid, M., Garfinkel, A. C. & Seidman, C. E. Differentiation and Contractile Analysis of GFP-Sarcomere Reporter hiPSC-Cardiomyocytes. *Curr Protoc Hum Genet* **96**, 21.12.1-21.12.12 (2018).

138. Maddah, M. *et al.* A non-invasive platform for functional characterization of stem-cell-derived cardiomyocytes with applications in cardiotoxicity testing. *Stem Cell Reports* **4**, 621–631 (2015).

139. Psaras, Y. *et al.* CalTrack: High-Throughput Automated Calcium Transient Analysis in Cardiomyocytes. *Circ Res* **129**, 326–341 (2021).

140. Yang, H. *et al.* Deriving waveform parameters from calcium transients in human iPSC-derived cardiomyocytes to predict cardiac activity with machine learning. *Stem Cell Reports* **17**, 556–568 (2022).

141. Shroff, S. N. *et al.* Voltage Imaging of Cardiac Cells and Tissue Using the Genetically Encoded Voltage Sensor Archon1. *iScience* **23**, (2020).

142. Lopaschuk, G. D., Spafford, M. A. & Marsh Cardiovascular, D. R. Glycolysis Is Predominant Source of Myocardial ATP Production Immediately after Birth. *Am J Physiol* **216**, 1698–1705 (1991).

143. Murashige, D. *et al.* Comprehensive quantification of fuel use by the failing and nonfailing human heart. *Science* (1979) **370**, 364–368 (2020).

144. Bhute, V. J. *et al.* Metabolomics identifies metabolic markers of maturation in human pluripotent stem cell-derived cardiomyocytes. *Theranostics* **7**, 2078–2091 (2017).

145. Yang, X. *et al.* Fatty Acids Enhance the Maturation of Cardiomyocytes Derived from Human Pluripotent Stem Cells. *Stem Cell Reports* **13**, 657–668 (2019).

146. Horikoshi, Y. *et al.* Fatty acid-treated induced pluripotent stem cell-derived human cardiomyocytes exhibit adult cardiomyocyte-like energy metabolism phenotypes. *Cells* **8**, (2019).

147. Zhang, J. Z. *et al.* A Human iPSC Double-Reporter System Enables Purification of Cardiac Lineage Subpopulations with Distinct Function and Drug Response Profiles. *Cell Stem Cell* **24**, 802–811 (2019).

148. Da Rocha, A. M. *et al.* HiPSC-CM Monolayer Maturation State Determines Drug Responsiveness in High Throughput Pro-Arrhythmia Screen. *Sci Rep* **7**, (2017).

149. Huebsch, N. *et al.* Metabolically driven maturation of human-induced-pluripotent-stem-cell-derived cardiac microtissues on microfluidic chips. *Nat Biomed Eng* **6**, 372–388 (2022). An informative study utilizing microfluidic chips and metabolic maturation to improve the alignment and maturation of hiPSC-CMs.

150. Lemcke, H., Skorska, A., Lang, C. I., Johann, L. & David, R. Quantitative evaluation of the sarcomere network of human hiPSC-derived cardiomyocytes using single-molecule localization microscopy. *Int J Mol Sci* **21**, (2020).

151. Yang, B. *et al.* A Net Mold-Based Method of Biomaterial-Free Three-Dimensional Cardiac Tissue Creation. *Tissue Eng Part C Methods* **25**, 243–252 (2019).

152. Piccini, I., Rao, J., Seebohm, G. & Greber, B. Human pluripotent stem cell-derived cardiomyocytes: Genome-wide expression profiling of long-term *in vitro* maturation in comparison to human heart tissue. *Genom Data* **4**, 69–72 (2015).

153. Tsui, J. H. *et al.* Tunable electroconductive decellularized extracellular matrix hydrogels for engineering human cardiac microphysiological systems. *Biomaterials* **272**, (2021).

154. Guyette, J. P. *et al.* Bioengineering Human Myocardium on Native Extracellular Matrix. *Circ Res* **118**, 56–72 (2016).

155. Zhao, Y. *et al.* A Platform for Generation of Chamber-Specific Cardiac Tissues and Disease Modeling. *Cell* **176**, 913-927 (2019).

156. Pretorius, D. *et al.* Layer-By-Layer Fabrication of Large and Thick Human Cardiac Muscle Patch Constructs With Superior Electrophysiological Properties. *Front Cell Dev Biol* **9**, (2021).

157. Geng, L. *et al.* Rapid electrical stimulation increased cardiac apoptosis through disturbance of calcium homeostasis and mitochondrial dysfunction in human induced pluripotent stem cell-derived cardiomyocytes. *Cellular Physiology and Biochemistry* **47**, 1167–1180 (2018).

158. Dickerson, D. A. Advancing Engineered Heart Muscle Tissue Complexity with Hydrogel Composites. *Advanced Biology* (2022).

159. Tani, H. *et al.* Heart-derived collagen promotes maturation of engineered heart tissue. *Biomaterials* **299**, (2023).

160. Kaiser, N. J., Kant, R. J., Minor, A. J. & Coulombe, K. L. K. Optimizing Blended Collagen-Fibrin Hydrogels for Cardiac Tissue Engineering with Human iPSC-derived Cardiomyocytes. *ACS Biomater Sci Eng* **5**, 887–899 (2019).

161. Lv, W., Babu, A., Morley, M. P., Musunuru, K. & Guerraty, M. Resource of Gene Expression Data From a Multiethnic Population Cohort of Induced Pluripotent Cell-Derived Cardiomyocytes. *Circ Genom Precis Med* (2024).

162. Soepriatna, A. H. *et al.* Action potential metrics and automated data analysis pipeline for cardiotoxicity testing using optically mapped hiPSC-derived 3D cardiac microtissues. *PLoS One* **18**, (2023).

163. Olivetti, G. *et al.* Aging, Cardiac Hypertrophy and Ischemic Cardiomyopathy Do Not Affect the Proportion of Mononucleated and Multinucleated Myocytes in the Human Heart. *Journal of Molecular and Cellular Cardiology* **28**, (1996).

164. Squire, J. M. Architecture and Function in the Muscle Sarcomere. *Curr Opin Struct Biol* **7**, 247-257 (1997).

165. Martin Gerdes, A. *et al.* Structural Remodeling of Cardiac Myocytes in Patients With Ischemic Cardiomyopathy. *Circulation* **86**, 426-430 (1992).

166. Feric, N. T. & Radisic, M. Maturing human pluripotent stem cell-derived cardiomyocytes in human engineered cardiac tissues. *Advanced Drug Delivery Reviews* **96**, 110–134 (2016).

167. Porter, G. A. *et al.* Bioenergetics, mitochondria, and cardiac myocyte differentiation. *Prog Pediatr Cardiol* **31**, 75–81 (2011).

168. Nagueh, S. F. *et al.* Altered titin expression, myocardial stiffness, and left ventricular function in patients with dilated cardiomyopathy. *Circulation* **110**, 155–162 (2004).

169. Van Der Velden, J. *et al.* Isometric Tension Development and Its Calcium Sensitivity in Skinned Myocyte-Sized Preparations from Different Regions of the Human Heart. *Cardiovascular Research* **42**, (1999).

170. Hasenfuss, G. *et al.* Energetics of Isometric Force Development in Control and Volume-Overload Human Myocardium Comparison With Animal Species. *Circ Res* **68**, 836-846 (1990).

171. Tenreiro, M. F., Louro, A. F., Alves, P. M. & Serra, M. Next generation of heart regenerative therapies: progress and promise of cardiac tissue engineering. *npj Regenerative Medicine* **6**, (2021).

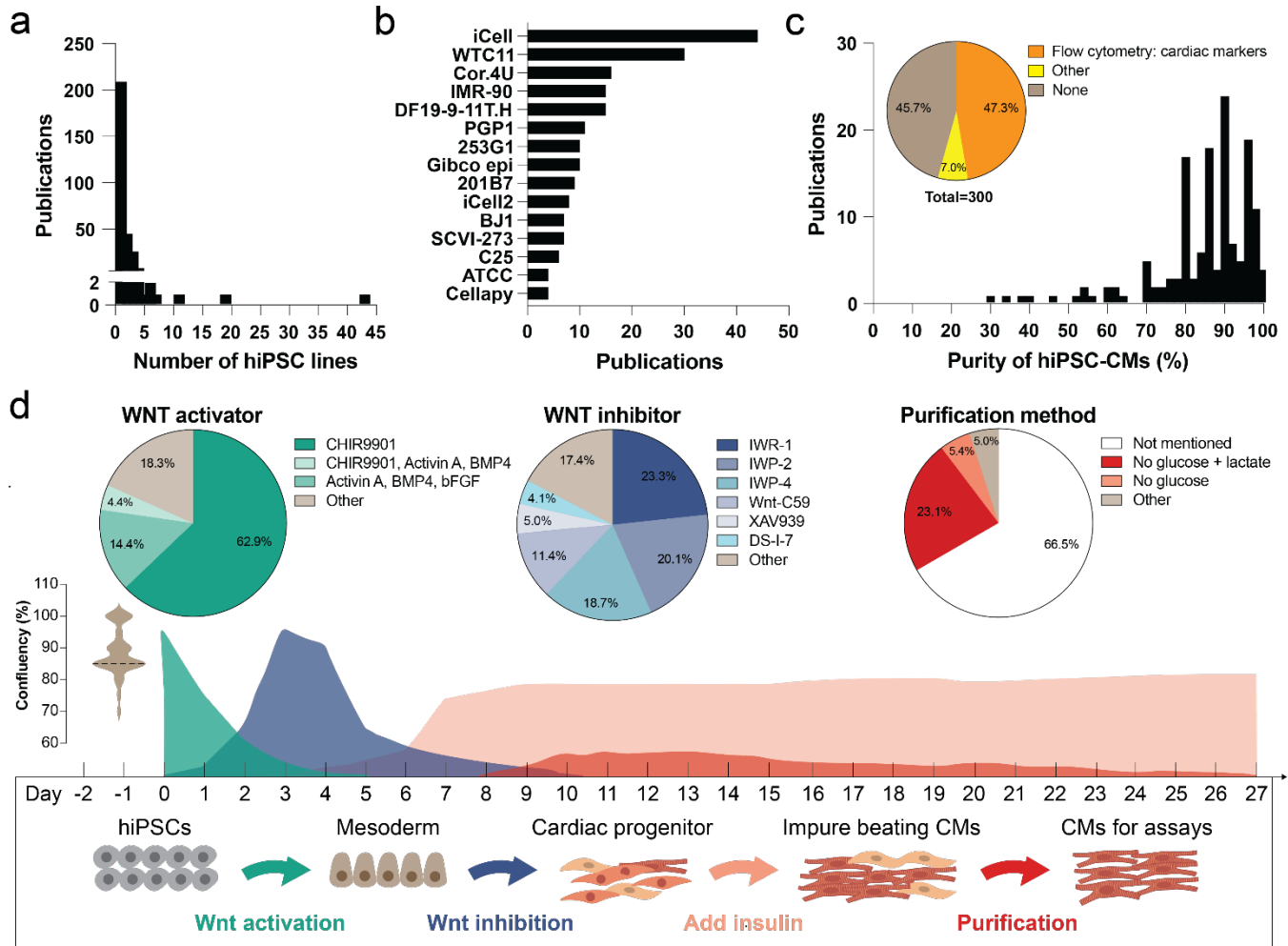
172. Drouin, E., Charpentier, F., Gauthier, C., Laurent, K. & Le Marec, H. Electrophysiologic characteristics of cells spanning the left ventricular wall of human heart: Evidence for presence of M cells. *J Am Coll Cardiol* **26**, 185–192 (1995).

173. Koncz, I. *et al.* Electrophysiological effects of ivabradine in dog and human cardiac preparations: Potential antiarrhythmic actions. *Eur J Pharmacol* **668**, 419–426 (2011).

174. Dangman, K. H. *et al.* Electrophysiologic Characteristics of Human Ventricular and Purkinje Fibers. *Circulation* **65**, 362-368 (1982).

175. Carafoli, E., Santella, L., Branca, D. & Brini, M. Generation, control, and processing of cellular calcium signals. *Critical Reviews in Biochemistry and Molecular Biology* **36**, 107–260 (2001).

## Figures



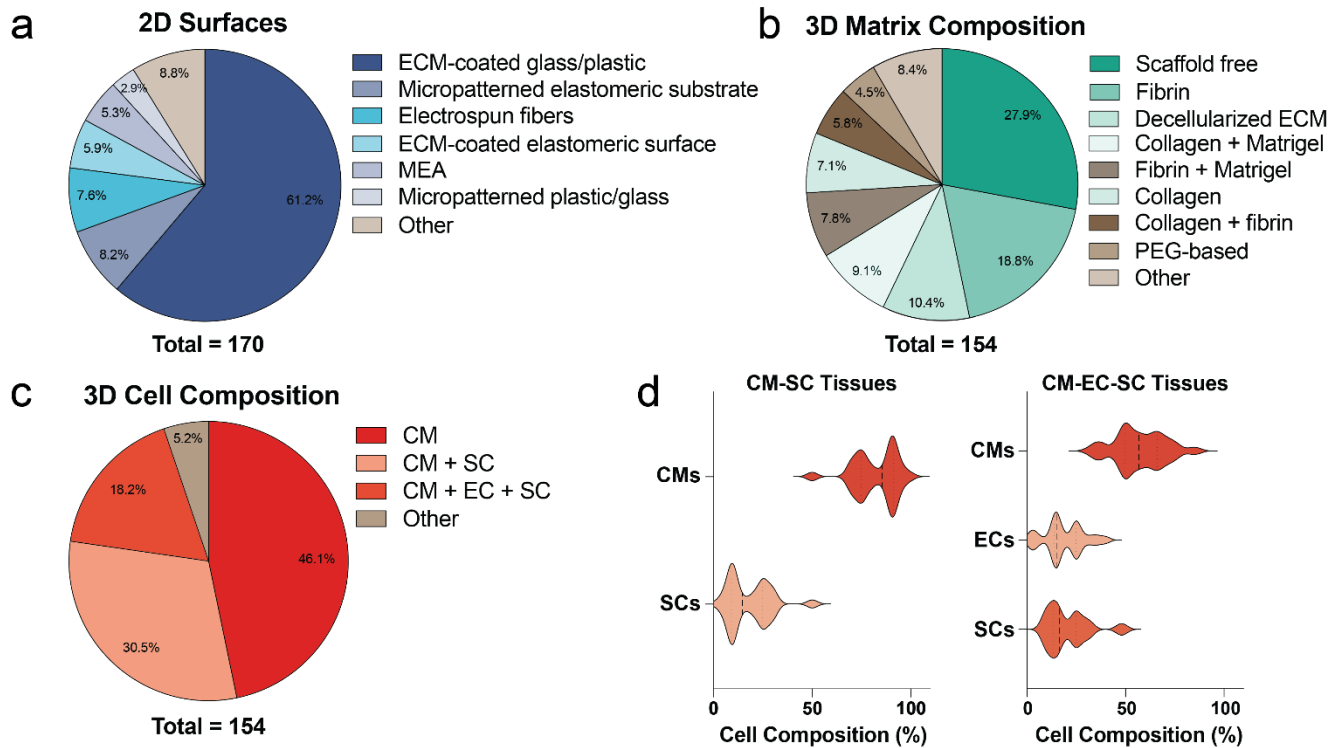


**Figure 2.** Variability in hiPSC-CM platforms. a. Top types of substrate platforms that hiPSC-CMs are seeded on in 2D. Multielectrode array (MEA). b. Top extracellular matrix (ECM) or biomaterial platform used to engineer cardiac microtissues. Polyethylene glycol (PEG). c. Fraction of cardiac microtissues that are composed of hiPSC-CMs alone (CM), hiPSC-CMs with mesenchymal stromal cells (CM + SC), or hiPSC-CMs with endothelial cells and mesenchymal stromal cells (CM + EC + SC). d. Left: Distribution of CM and SC composition in CM-SC cardiac microtissues (n = 50). Right: Distribution of CM, EC, and SC composition in CM-EC-SC cardiac microtissues (n = 26). Dashed and dotted lines represent medians and quartiles, respectively.

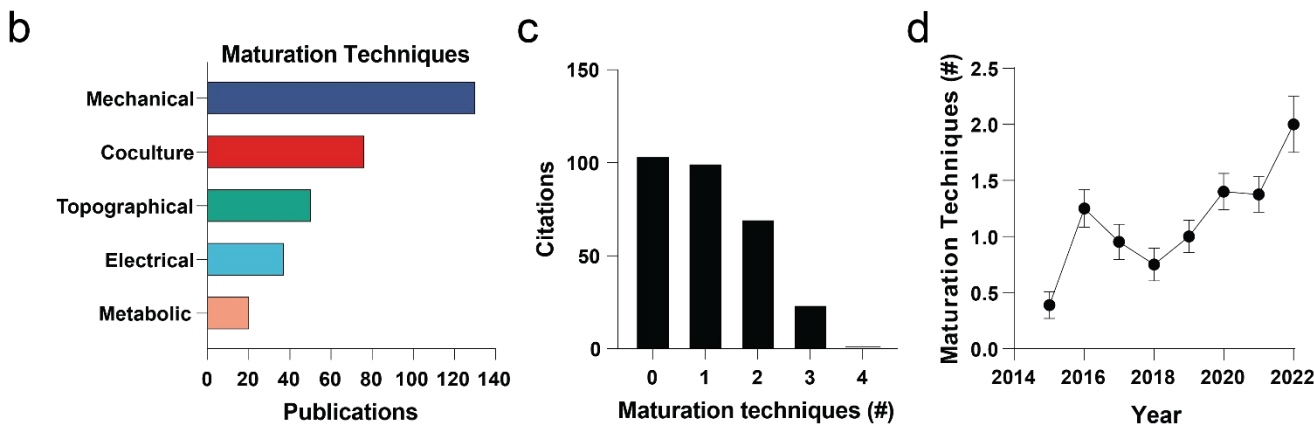
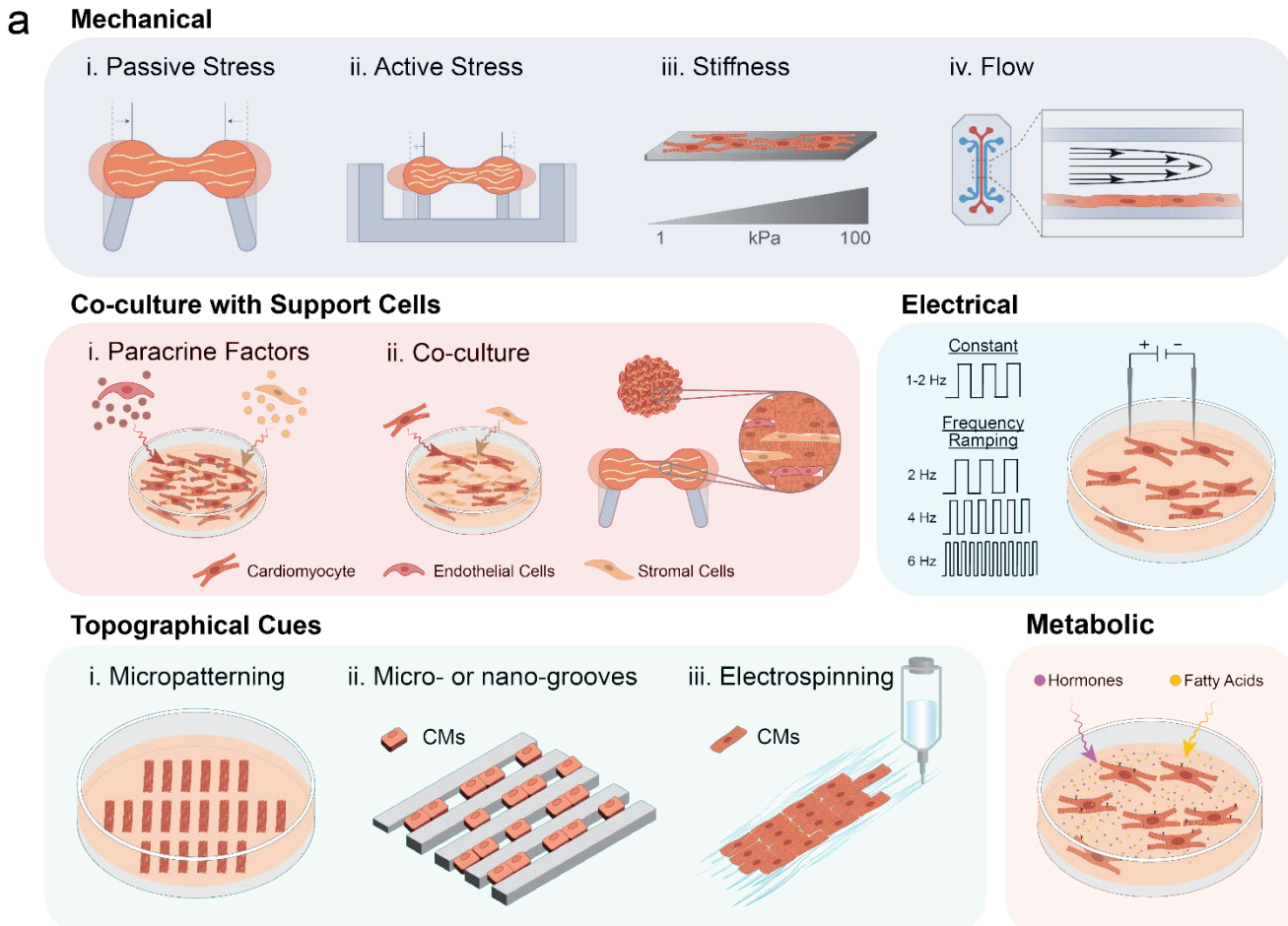


**Figure 3.** Maturation techniques used in hiPSC-CM culture. **a.** Schematic of types of maturation techniques, including mechanical, metabolic, co-culture, electrical stimulation, and alignment cues. **b.** Number of publications that reported using the listed maturation techniques. **c.** Histogram of the number of maturation techniques that the analyzed publications reported. **d.** Average number of maturation techniques reported over time (n = 18-34). Error bars are standard error of the mean (SEM).

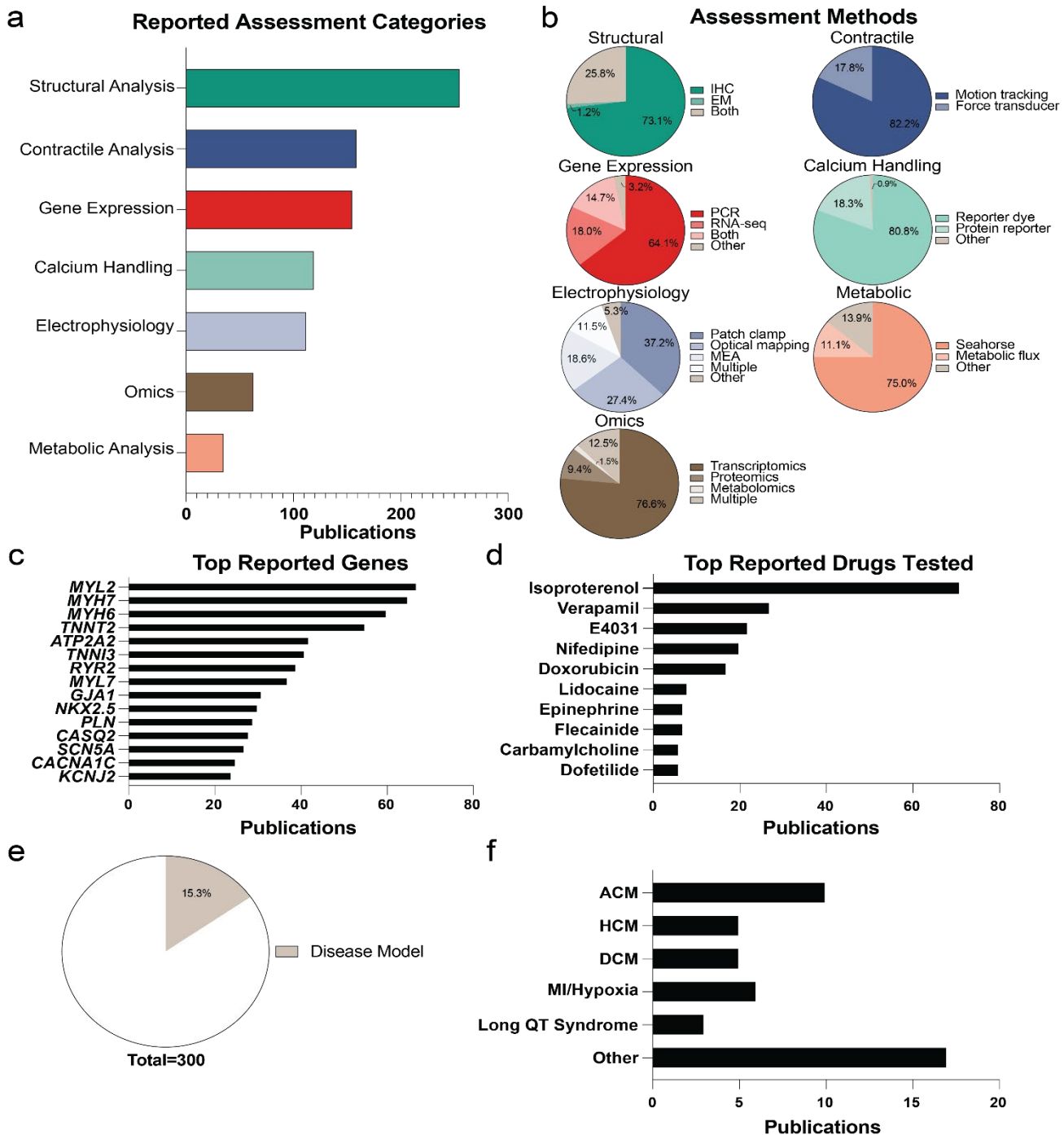


**Figure 4.** Methods of assessing hiPSC-CM functionality and maturation. a. Number of publications that reported analysis of the structure, contraction, gene expression, calcium handling, electrophysiology, and metabolism of hiPSC-CMs. b. Top methods of obtaining each of the reported metrics in a. c. Top genes that were reported in the assessment of hiPSC-CM maturation. d. Top pharmaceutical drugs used to test the ability of hiPSC-CMs to respond as known clinically. e. Proportion of publications that used hiPSC-CM platforms to model disease. f. Top diseases modeled by hiPSC-CM platforms including arrhythmogenic cardiomyopathy (ACM), hypertrophic cardiomyopathy (HCM), dilated cardiomyopathy (DCM), myocardial infarction (MI), and long QT syndrome (LQT).

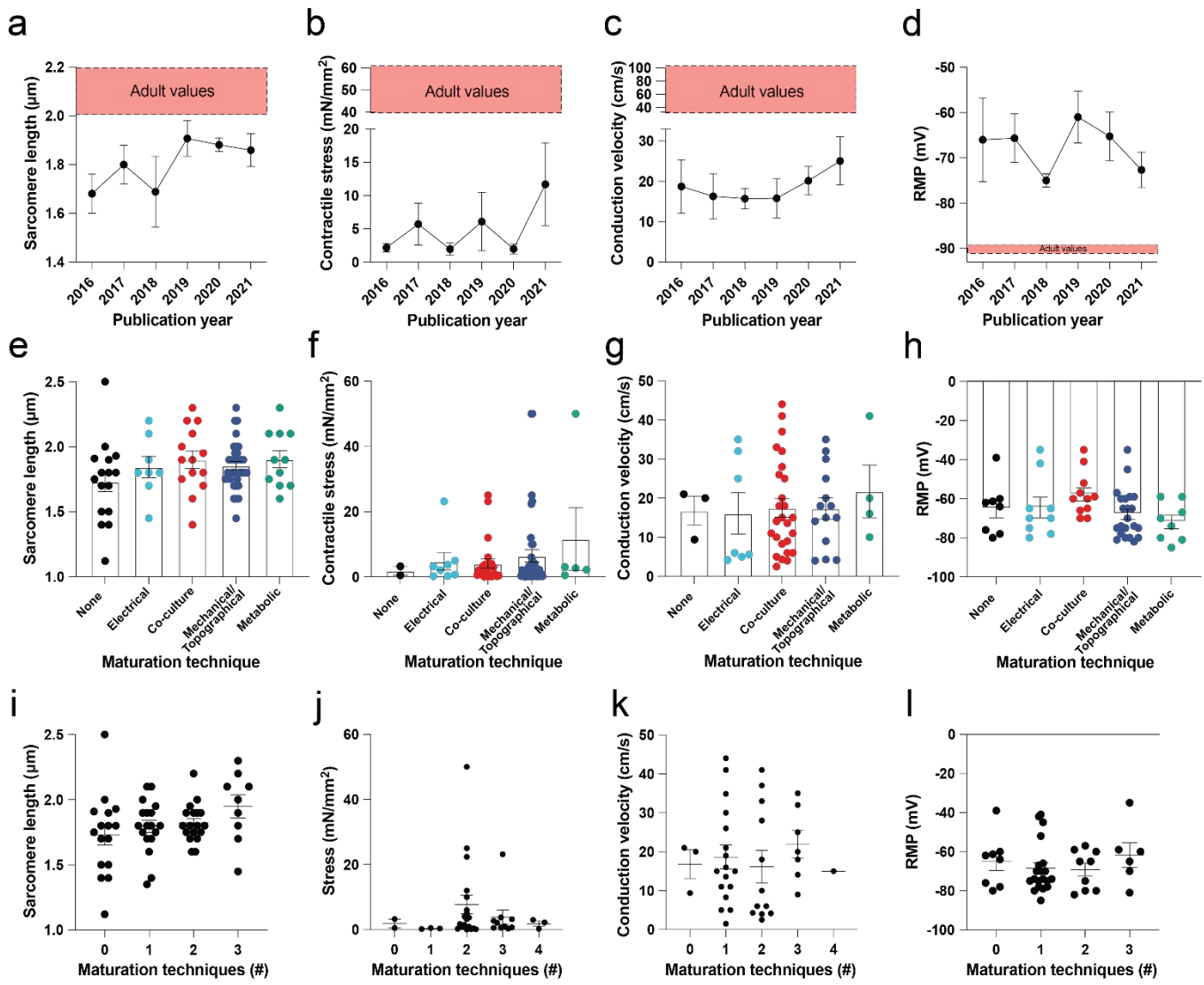


**Figure 5.** Quantification of hiPSC-CM functionality and maturation. **a-d.** Average reported sarcomere length, contractile stress, conduction velocity (CV), and resting membrane potential (RMP) in hiPSC-CMs each year from 2016-2021 ( $n = 4-11$ ). 2015 and 2022 were excluded from these graphs due to limited data availability (analysis was performed mid-2022). Red regions represent values benchmarked in adult human CMs. **e-h.** Average reported metrics based on types of maturation techniques that were used from all analyzed publications ( $n = 2-34$ ). **i-l.** Average reported metrics based on the number of maturation techniques that were used from all analyzed publications ( $n = 2-20$ ). Maturation techniques were classified as described in Figure 3. Error bars are standard error of the mean (SEM).

**Table 1:** Adult cardiomyocyte benchmarking parameters and values.

<b>Benchmarking parameters and corresponding values of adult cardiomyocyte/tissue</b>	
<b>Structural Organization</b>	<ul style="list-style-type: none"> <li>• Rod-shaped with aligned, developed myofibrils</li> <li>• Binucleated<sup>163</sup></li> <li>• Sarcomere length: ~ 2.0 – 2.2 <math>\mu\text{m}</math><sup>164,165</sup></li> <li>• Cardiomyocyte surface area: ~ 10,000-14,000 <math>\mu\text{m}^2</math><sup>166</sup></li> <li>• T-tubules present</li> <li>• Mitochondria localized near sarcomere<sup>167</sup></li> <li>• Expression of adult ventricular CM-specific structural genes (i.e. <i>MYH7</i>, <i>MYL2</i>, <i>TNNI3</i>, etc.)</li> </ul>
<b>Mechanical Properties</b>	<ul style="list-style-type: none"> <li>• Tissue elastic modulus ~10 – 50 kPa<sup>168</sup></li> </ul>
<b>Force</b>	<ul style="list-style-type: none"> <li>• Contractile stress: ~ 30 – 60 mN/mm<sup>2</sup><sup>169,170</sup></li> <li>• Positive force-frequency ratio</li> </ul>
<b>Electrophysiology</b>	<ul style="list-style-type: none"> <li>• Low to zero spontaneous contractions<sup>24,171</sup></li> <li>• Characteristic notch at the top of upstroke<sup>166</sup></li> <li>• Resting membrane potential: ~ -90 mV<sup>172</sup></li> <li>• Action potential amplitude: ~ 100-110 mV<sup>173</sup></li> <li>• Action potential duration: ~ 230-300 ms<sup>174</sup></li> <li>• Depolarization velocity: ~ 250- 300 V/s<sup>173</sup></li> <li>• Conduction velocity: ~ 30-100 cm/s<sup>25</sup></li> </ul>
<b>Calcium Conduction</b>	<ul style="list-style-type: none"> <li>• Cytosolic <math>\text{Ca}^{2+}</math> concentration<sup>175</sup>: <ul style="list-style-type: none"> <li>○ Resting ~100 nM</li> <li>○ Post SR calcium release ~1 <math>\mu\text{M}</math></li> </ul> </li> <li>• Mature sarcoplasmic reticulum function</li> <li>• Increased gene expression of calcium handling machinery <i>CACNA1C</i>, <i>SCN5A</i>, <i>KCND3</i>, <i>KCNJ2</i>, <i>SLC8A</i>, <i>ATP2A2</i>, <i>CASQ2</i>, <i>RYR2</i>, <i>GJA1</i>, <i>PLN</i></li> <li>• Robust organization of calcium handling machinery</li> </ul>
<b>Metabolic Maturity</b>	<ul style="list-style-type: none"> <li>• Reliant mainly on fatty acid oxidation: &gt;70%<sup>142,143</sup></li> <li>• Reduction in glycolysis: &lt; 10% of total energy source<sup>142</sup></li> <li>• Mitochondrial volume: ~30% of cell volume<sup>24</sup></li> </ul>